Gravitational Wave Data Analysis

Hyung Won Lee, Jeongcho Kim(Inje University)
and Chunglee Kim(Ewha University)

NR Workshop

January 10, 2020, Ewha, Seoul

based on data extraction (arXiv:1908.11170) and parameter estimation (PRD91.042003)

Contents

- Introduction
- Properties of LIGO-Virgo data
- Basic properties of detector noise
- Fourier domain analysis
- Time-frequency analysis and stationarity
- Detector calibration and data quality
- Noise model and likelihood
- Signal detection
- Inferring waveform and physical parameters
- Residuals analysis of LIGO data around GW150914
- Conclusions

Gravitational Waves

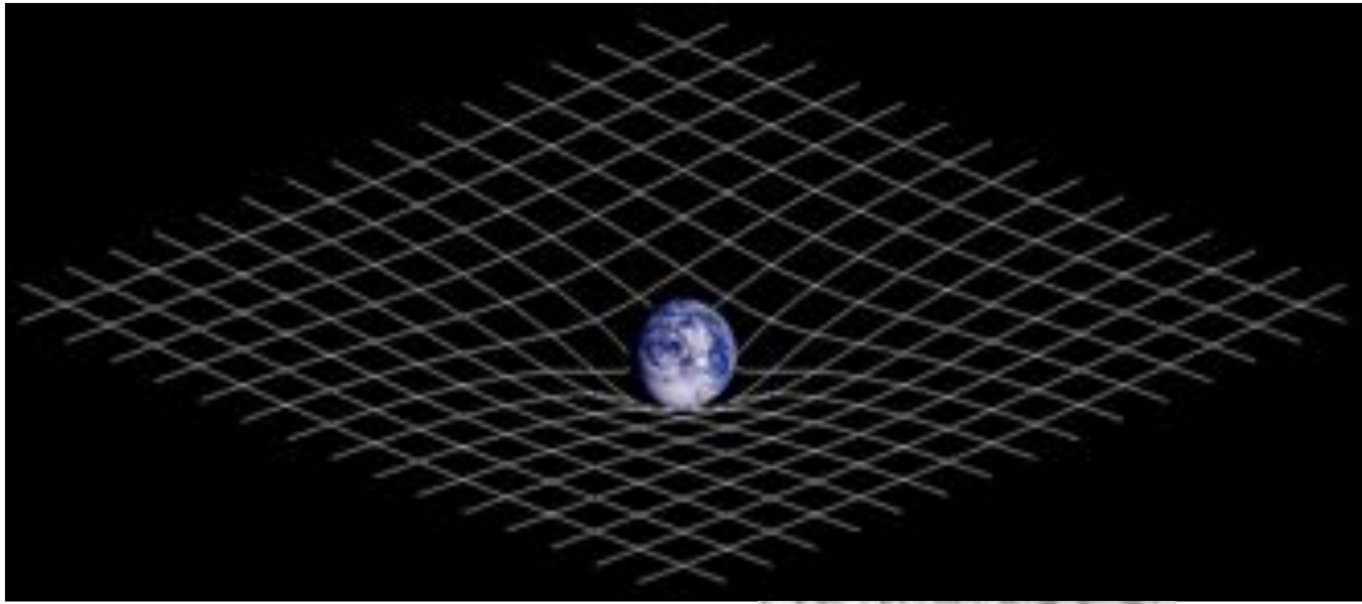

- Linearized Einstein Equation
- $g_{\mu\nu} = \eta_{\mu\nu} + h_{\mu\nu},\ \left|h_{\mu\nu}\right| \ll 1$
- $G_{\mu\nu} = \frac{8\pi G}{c^4} T_{\mu\nu}$
- $\eta^{\alpha\beta}\partial_\alpha\partial_\beta h_{\mu\nu} + O(h^2) = -\frac{16\pi G}{c^4} T_{\mu\nu},\ \partial^\mu h_{\mu\nu} = 0$
- Wave equation
- $\eta^{\alpha\beta}\partial_\alpha\partial_\beta h_{\mu\nu} = 0 \qquad h_{\mu\nu} = \frac{2G}{Rc^4}\ddot{I}_{\mu\nu}$

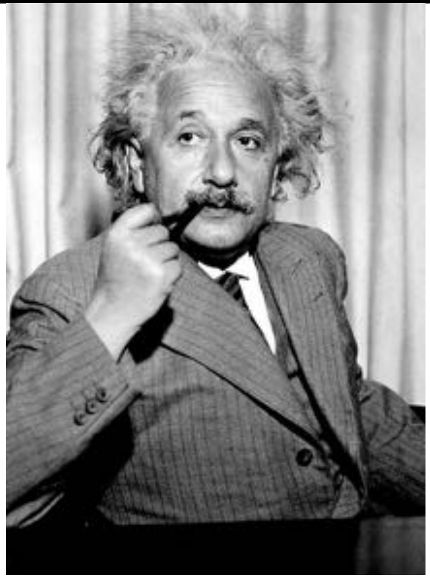

Gravitational Waves

- $\eta^{\alpha\beta}\partial_\alpha\partial_\beta h_{\mu\nu} = -\frac{16\pi G}{c^4}\tau_{\mu\nu}$
- $h^{\mu\nu}(t,\vec{x}) = \frac{G}{c^4}\int \frac{\tau^{\mu\nu}\left(t-\frac{\|\vec{x}-\vec{y}\|}{c},\vec{y}\right)}{\|\vec{x}-\vec{y}\|} d^3y$
- Far Zone
  $h^{ij}(t,\vec{x}) \approx \frac{2G}{rc^4}\ddot{I}\left(t-\frac{r}{c}\right)$

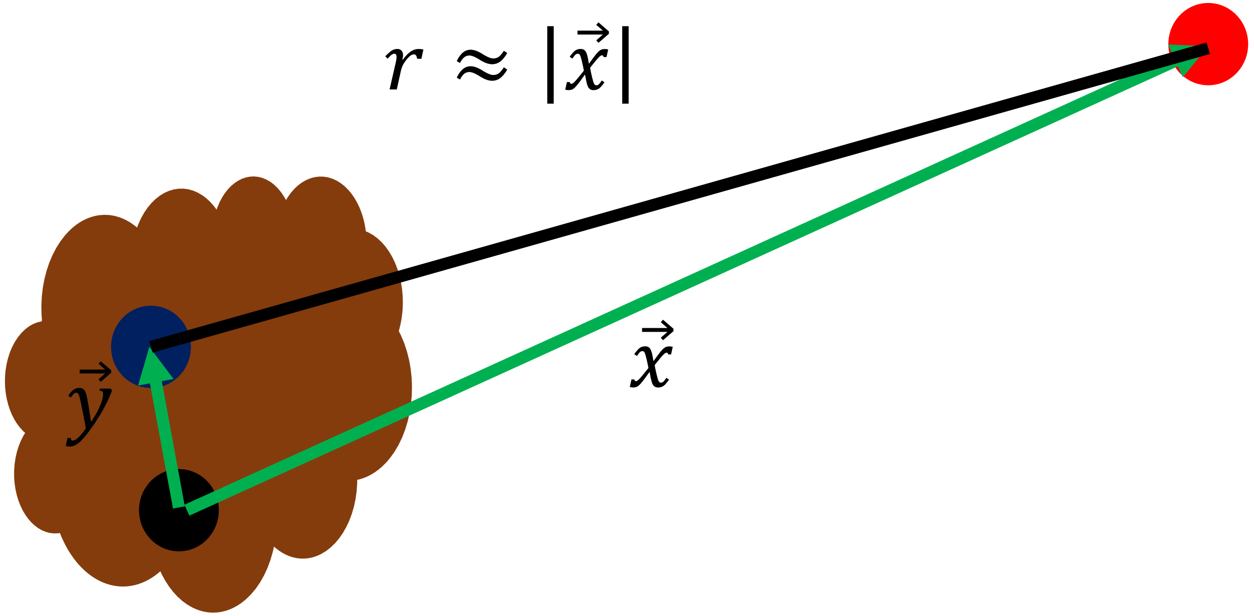

Existence of Gravitational Waves

- Indirect proof with pulsar observation
- Nobel Prize in Physics at 1993
- First direct detection at 2015 Sep. 14

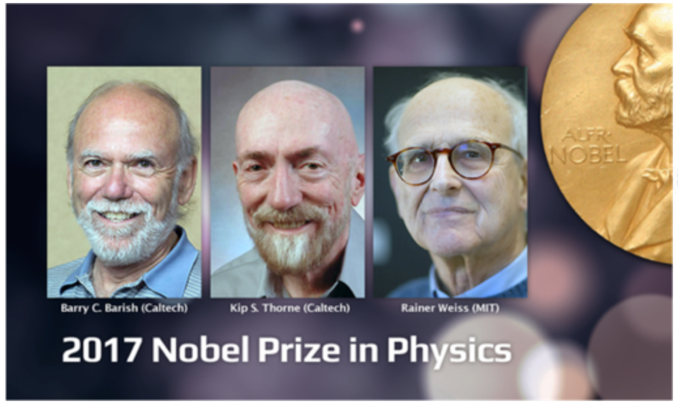

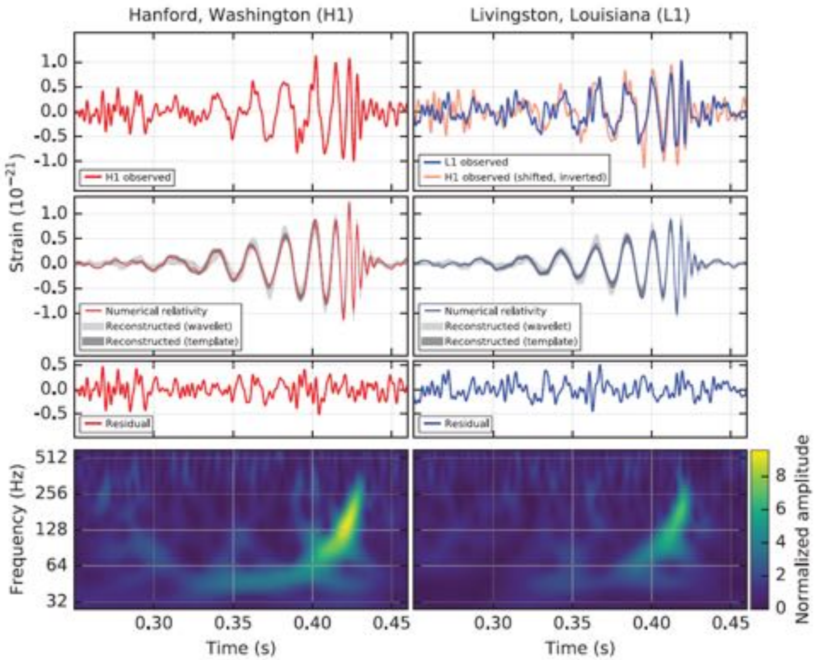

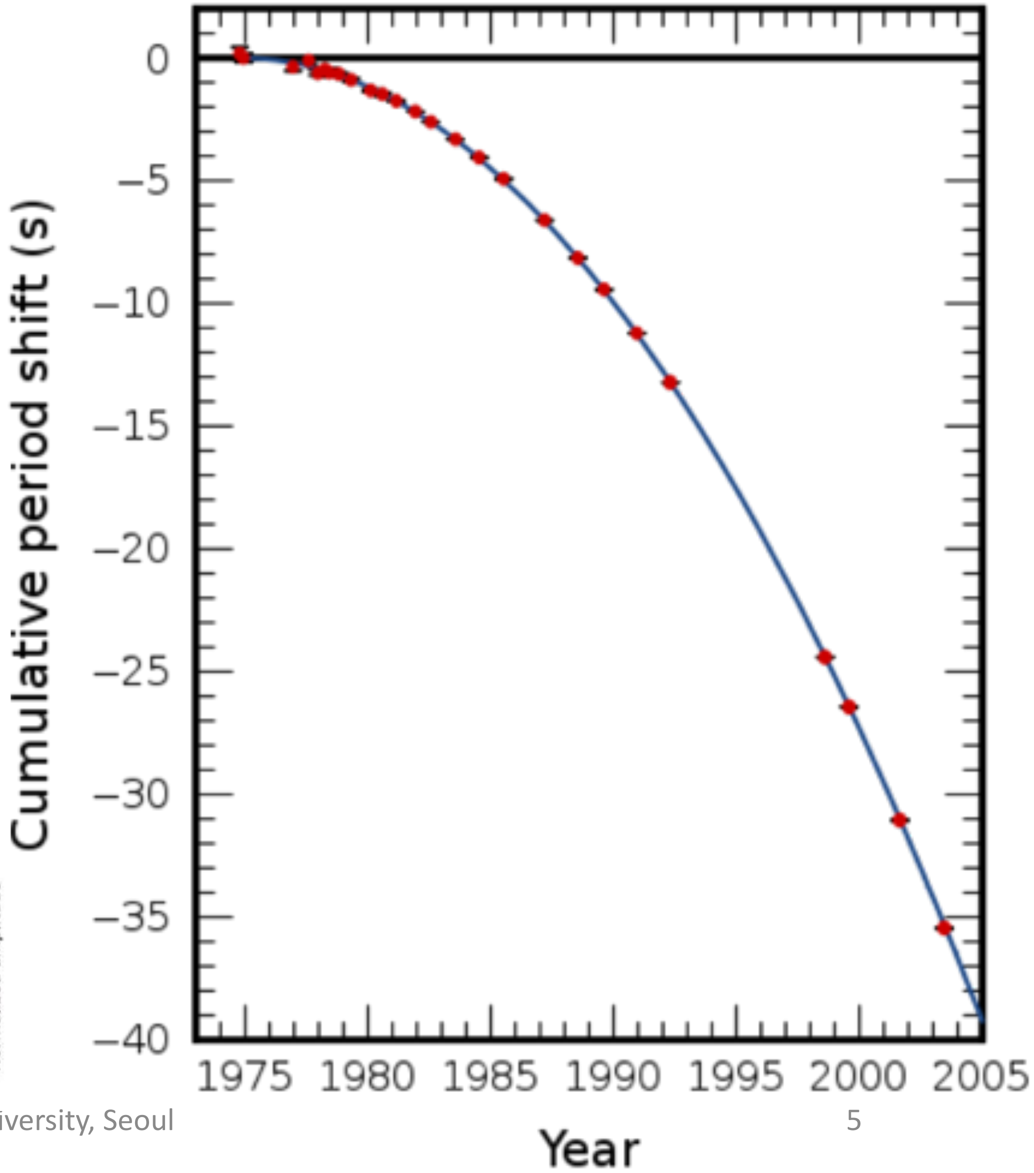

Introduction

- Open a new window to observe the Universe

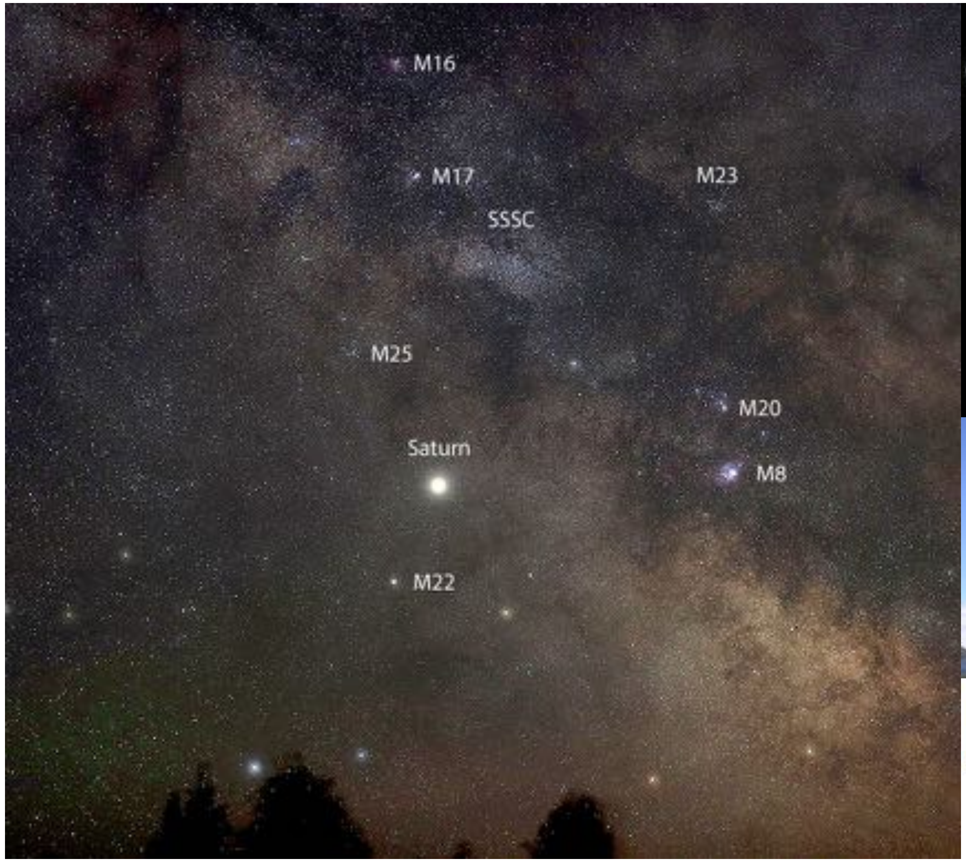

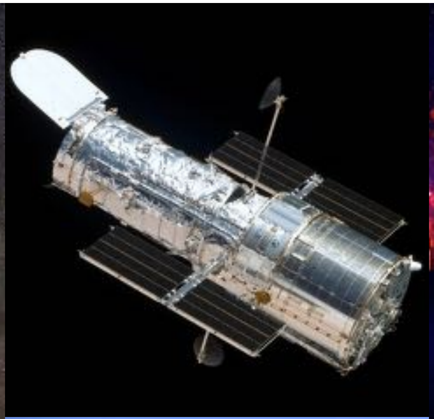


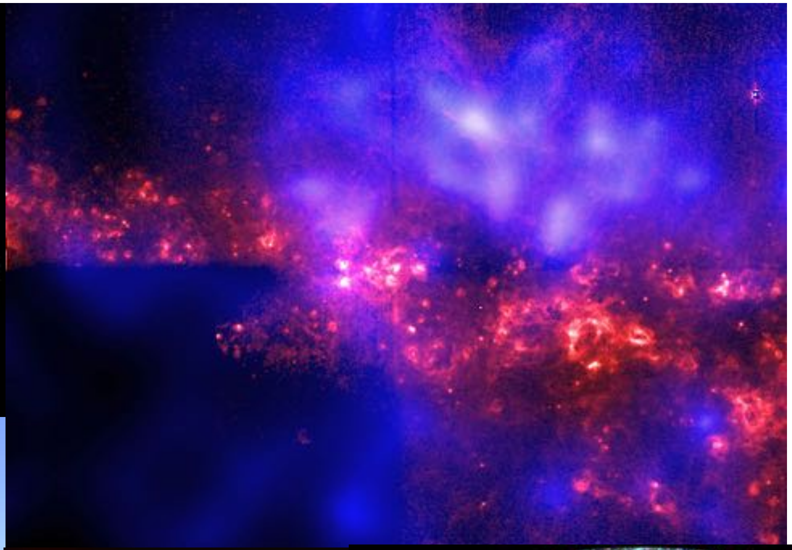

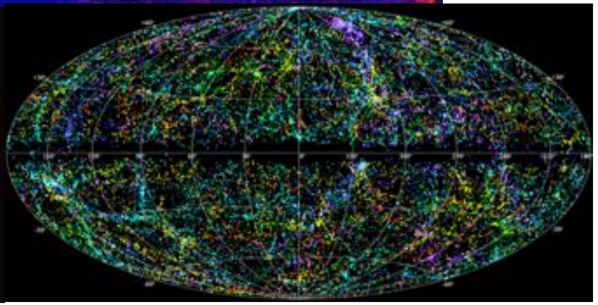

Global Detector Network

Observational runs

- Observing runs
  - O1 : aLIGO 2015/09/12 – 2016/01/19
  - O2 : aLIGO 2016/11/30 – 2017/08/25
  - Adv. Virgo joined 2017/08/01
- Coincident analysis time : 166.6 days
  - O1 : 48.6 days
  - O2 : 118 days
- O2 data were recalibrated and cleaned
- O3 2019/04/01 ~ current
  L1 : 140Mpc, H1 : 120Mpc, V1 : 50Mpc

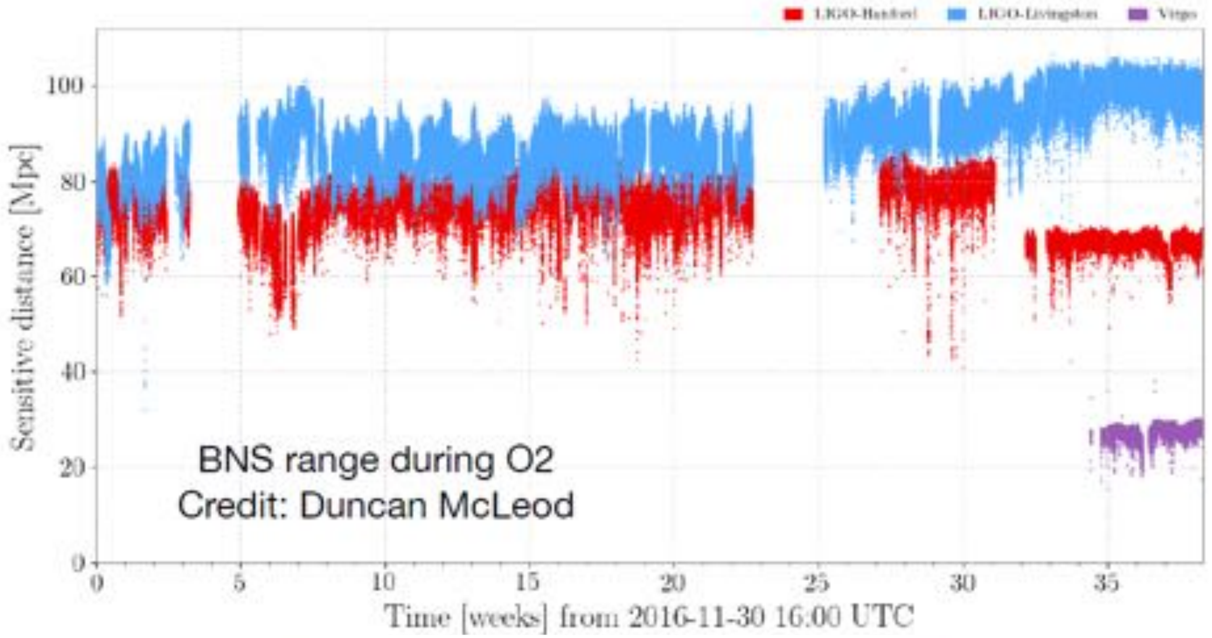

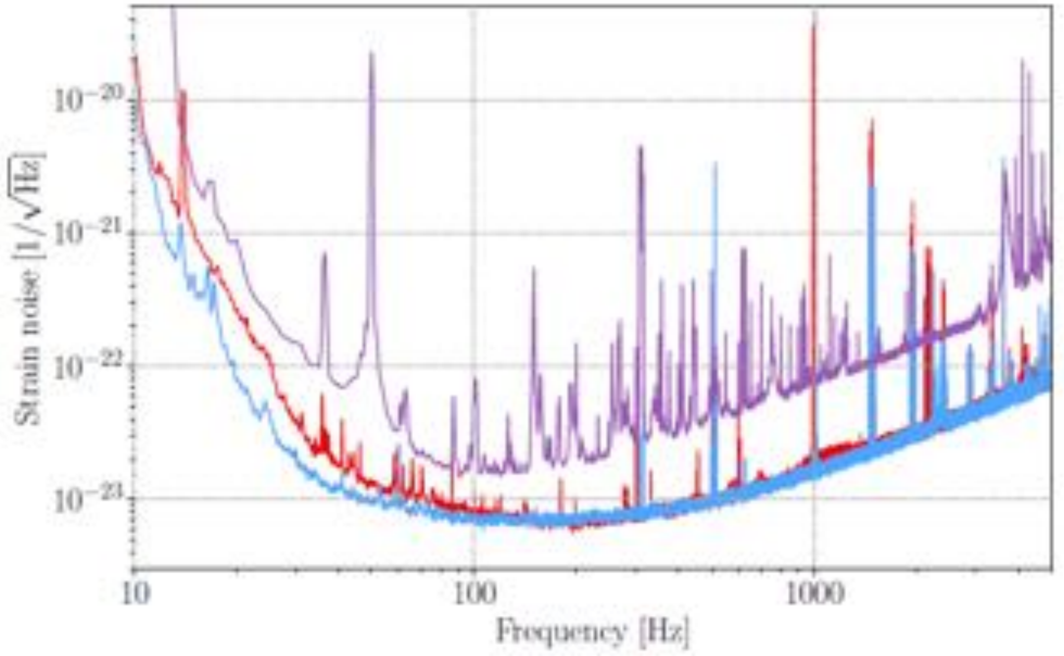

O1/O2 observation results

Event	$m_1/\mathrm{M}_\odot$	$m_2/\mathrm{M}_\odot$	$\mathcal{M}/\mathrm{M}_\odot$	χ_{eff}	$M_f/\mathrm{M}_\odot$	a_f	$E_{\mathrm{rad}}/(\mathrm{M}_\odot c^2)$	$\ell_{\mathrm{peak}}/(\mathrm{erg\,s^{-1}})$	d_L/Mpc	z	$\Delta\Omega/\mathrm{deg}^2$
GW150914	$35.6^{+4.8}_{-3.0}$	$30.6^{+3.0}_{-4.4}$	$28.6^{+1.6}_{-1.5}$	$-0.01^{+0.12}_{-0.13}$	$63.1^{+3.3}_{-3.0}$	$0.69^{+0.05}_{-0.04}$	$3.1^{+0.4}_{-0.4}$	$3.6^{+0.4}_{-0.4}\times10^{56}$	430^{+150}_{-170}	$0.09^{+0.03}_{-0.03}$	180
GW151012	$23.3^{+14.0}_{-5.5}$	$13.6^{+4.1}_{-4.8}$	$15.2^{+2.0}_{-1.1}$	$0.04^{+0.28}_{-0.19}$	$35.7^{+9.9}_{-3.8}$	$0.67^{+0.13}_{-0.11}$	$1.5^{+0.5}_{-0.5}$	$3.2^{+0.8}_{-1.7}\times10^{56}$	1060^{+540}_{-480}	$0.21^{+0.09}_{-0.09}$	1555
GW151226	$13.7^{+8.8}_{-3.2}$	$7.7^{+2.2}_{-2.6}$	$8.9^{+0.3}_{-0.3}$	$0.18^{+0.20}_{-0.12}$	$20.5^{+6.4}_{-1.5}$	$0.74^{+0.07}_{-0.05}$	$1.0^{+0.1}_{-0.2}$	$3.4^{+0.7}_{-1.7}\times10^{56}$	440^{+180}_{-190}	$0.09^{+0.04}_{-0.04}$	1033
GW170104	$31.0^{+7.2}_{-5.6}$	$20.1^{+4.9}_{-4.5}$	$21.5^{+2.1}_{-1.7}$	$-0.04^{+0.17}_{-0.20}$	$49.1^{+5.2}_{-3.9}$	$0.66^{+0.08}_{-0.10}$	$2.2^{+0.5}_{-0.5}$	$3.3^{+0.6}_{-0.9}\times10^{56}$	960^{+430}_{-410}	$0.19^{+0.07}_{-0.08}$	924
GW170608	$10.9^{+5.3}_{-1.7}$	$7.6^{+1.3}_{-2.1}$	$7.9^{+0.2}_{-0.2}$	$0.03^{+0.19}_{-0.07}$	$17.8^{+3.2}_{-0.7}$	$0.69^{+0.04}_{-0.04}$	$0.9^{+0.05}_{-0.1}$	$3.5^{+0.4}_{-1.3}\times10^{56}$	320^{+120}_{-110}	$0.07^{+0.02}_{-0.02}$	396
GW170729	$50.6^{+16.6}_{-10.2}$	$34.3^{+9.1}_{-10.1}$	$35.7^{+6.5}_{-4.7}$	$0.36^{+0.21}_{-0.25}$	$80.3^{+14.6}_{-10.2}$	$0.81^{+0.07}_{-0.13}$	$4.8^{+1.7}_{-1.7}$	$4.2^{+0.9}_{-1.5}\times10^{56}$	2750^{+1350}_{-1320}	$0.48^{+0.19}_{-0.20}$	1033
GW170809	$35.2^{+8.3}_{-6.0}$	$23.8^{+5.2}_{-5.1}$	$25.0^{+2.1}_{-1.6}$	$0.07^{+0.16}_{-0.16}$	$56.4^{+5.2}_{-3.7}$	$0.70^{+0.08}_{-0.09}$	$2.7^{+0.6}_{-0.6}$	$3.5^{+0.6}_{-0.9}\times10^{56}$	990^{+320}_{-380}	$0.20^{+0.05}_{-0.07}$	340
GW170814	$30.7^{+5.7}_{-3.0}$	$25.3^{+2.9}_{-4.1}$	$24.2^{+1.4}_{-1.1}$	$0.07^{+0.12}_{-0.11}$	$53.4^{+3.2}_{-2.4}$	$0.72^{+0.07}_{-0.05}$	$2.7^{+0.4}_{-0.3}$	$3.7^{+0.4}_{-0.5}\times10^{56}$	580^{+160}_{-210}	$0.12^{+0.03}_{-0.04}$	87
GW170817	$1.46^{+0.12}_{-0.10}$	$1.27^{+0.09}_{-0.09}$	$1.186^{+0.001}_{-0.001}$	$0.00^{+0.02}_{-0.01}$	≤ 2.8	≤ 0.89	≥ 0.04	$\geq 0.1\times10^{56}$	40^{+10}_{-10}	$0.01^{+0.00}_{-0.00}$	16
GW170818	$35.5^{+7.5}_{-4.7}$	$26.8^{+4.3}_{-5.2}$	$26.7^{+2.1}_{-1.7}$	$-0.09^{+0.18}_{-0.21}$	$59.8^{+4.8}_{-3.8}$	$0.67^{+0.07}_{-0.08}$	$2.7^{+0.5}_{-0.5}$	$3.4^{+0.5}_{-0.7}\times10^{56}$	1020^{+430}_{-360}	$0.20^{+0.07}_{-0.07}$	39
GW170823	$39.6^{+10.0}_{-6.6}$	$29.4^{+6.3}_{-7.1}$	$29.3^{+4.2}_{-3.2}$	$0.08^{+0.20}_{-0.22}$	$65.6^{+9.4}_{-6.6}$	$0.71^{+0.08}_{-0.10}$	$3.3^{+0.9}_{-0.8}$	$3.6^{+0.6}_{-0.9}\times10^{56}$	1850^{+840}_{-840}	$0.34^{+0.13}_{-0.14}$	1651

Released Gravitational-Wave Events

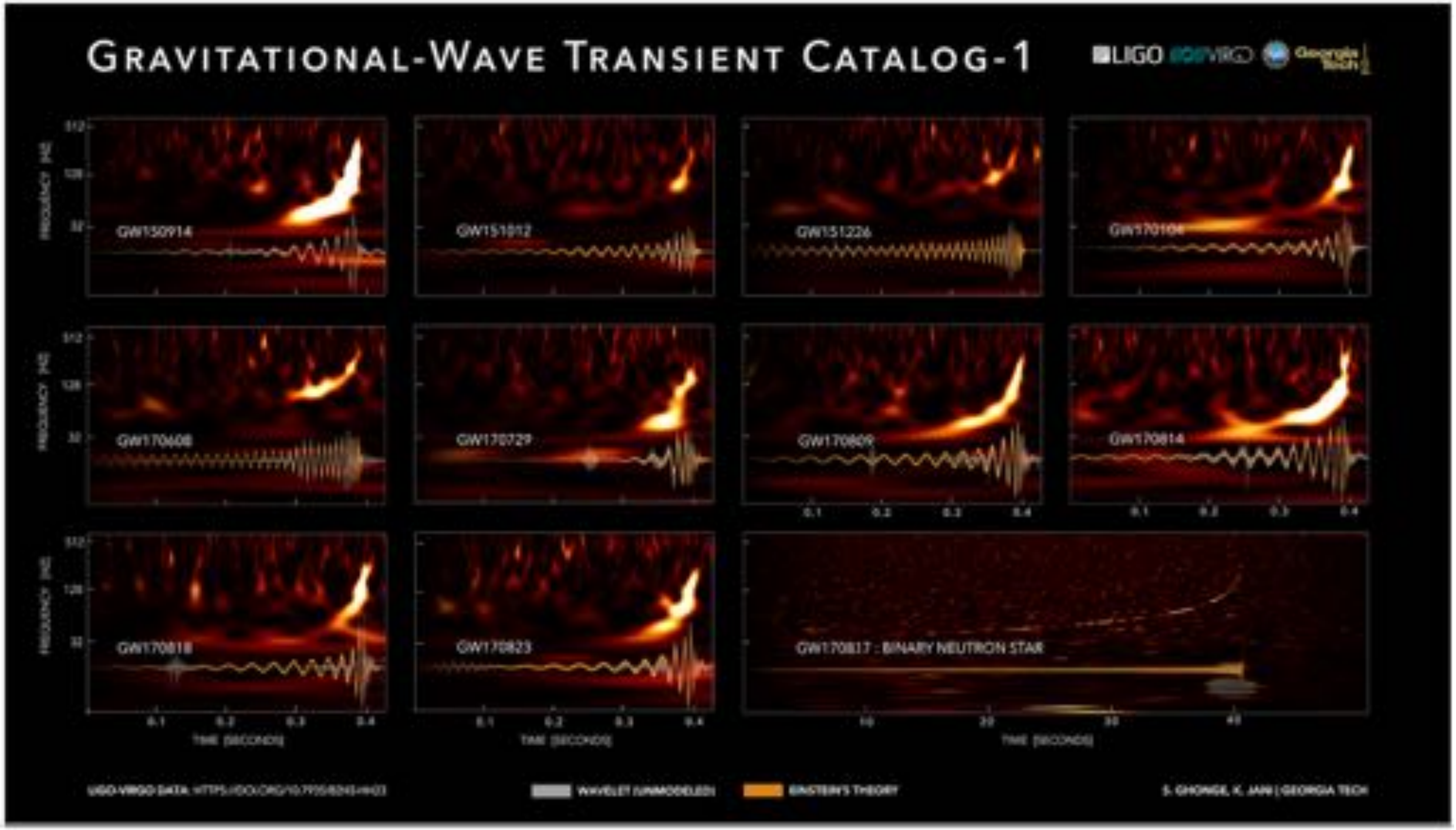

First BNS observation

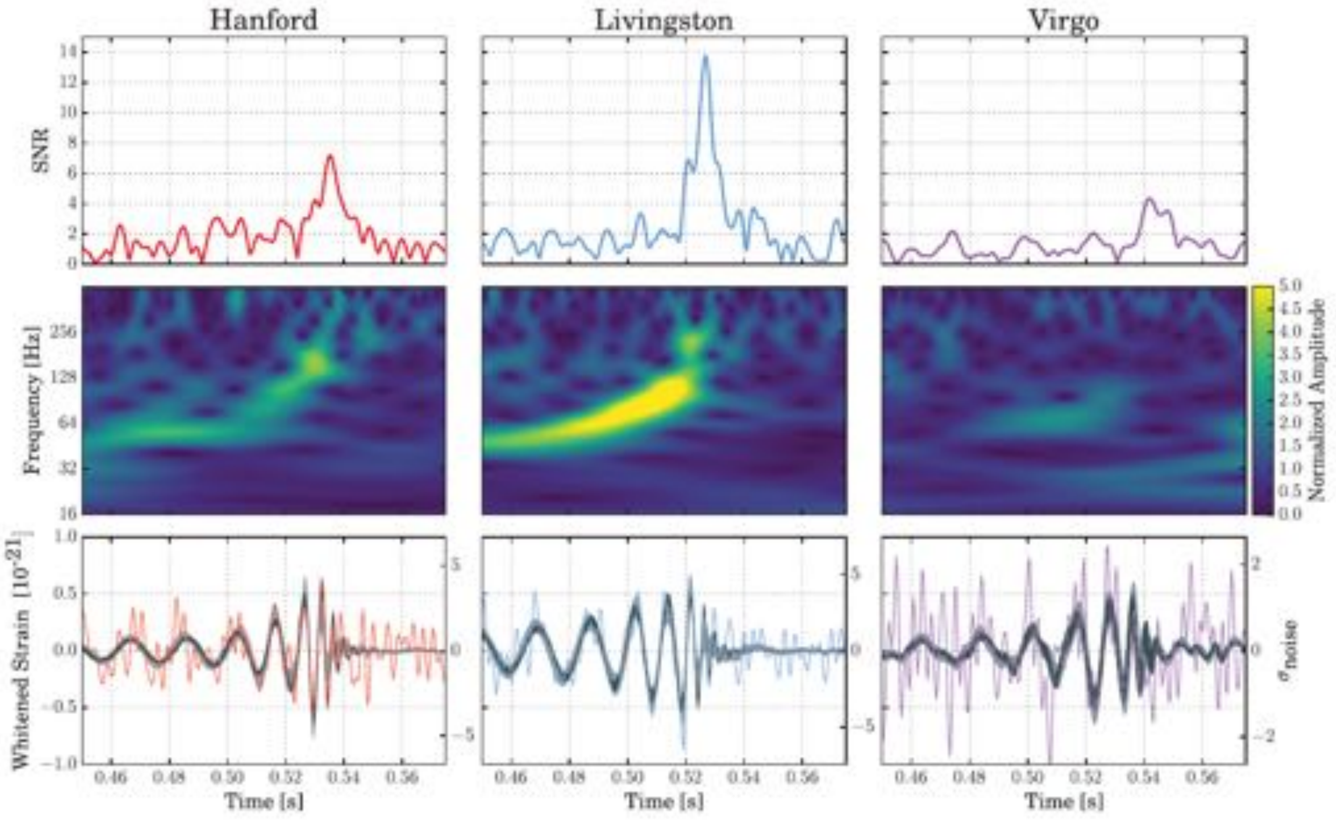

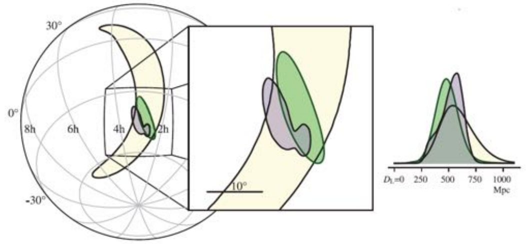

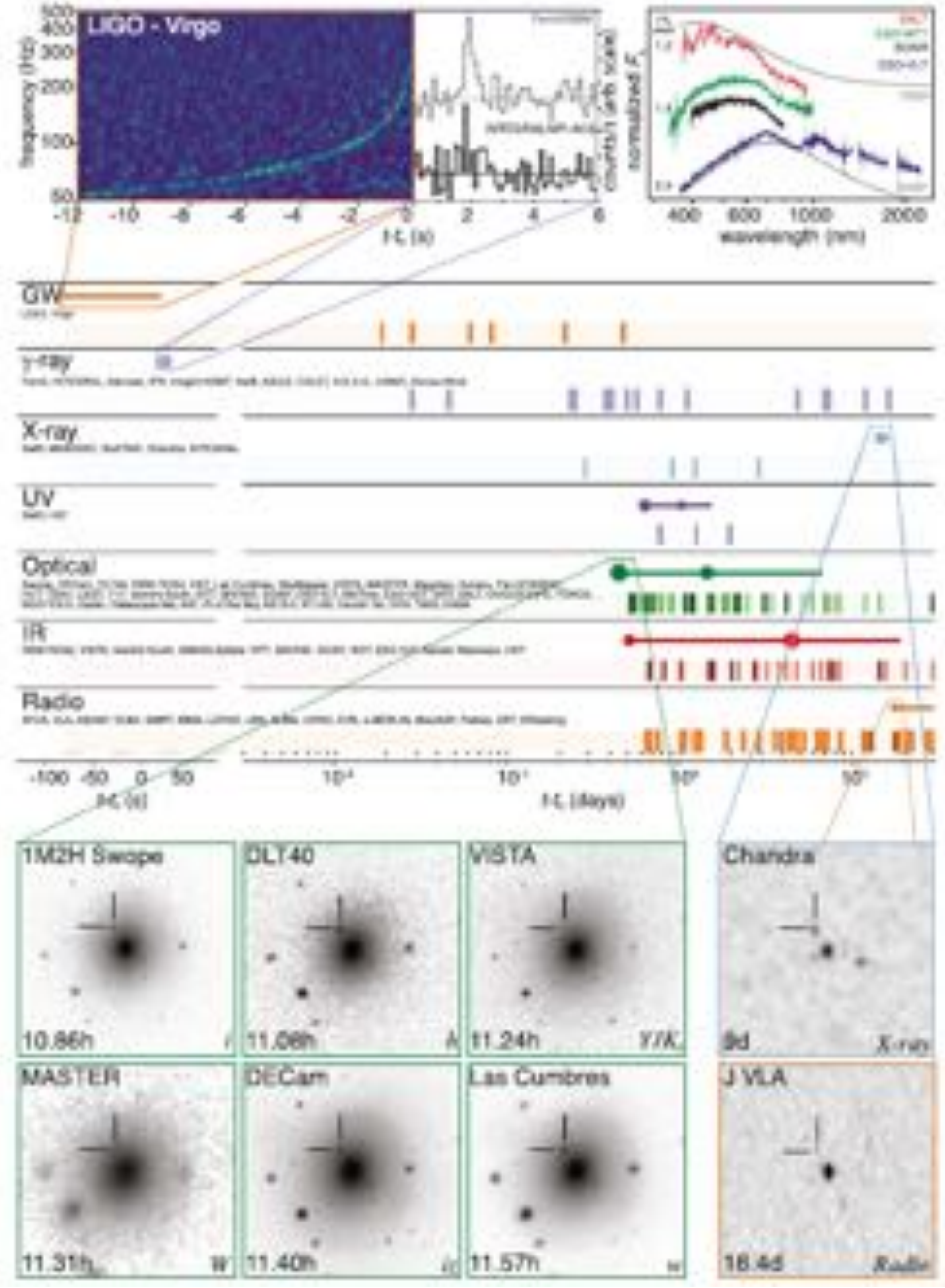

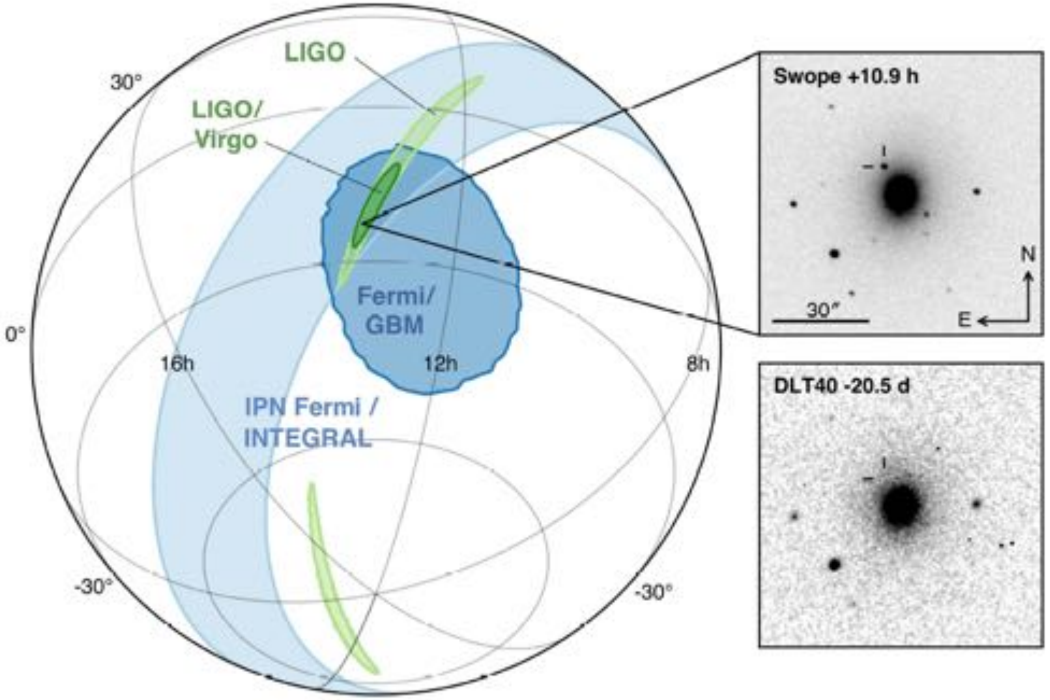

LIGO
30°
LIGO/
Virgo
Fermi/
GBM
0°
16h
12h
8h
IPN Fermi /
INTEGRAL
-30°
-30°
Swope +10.9 h
30″
N
E
DLT40 -20.5 d

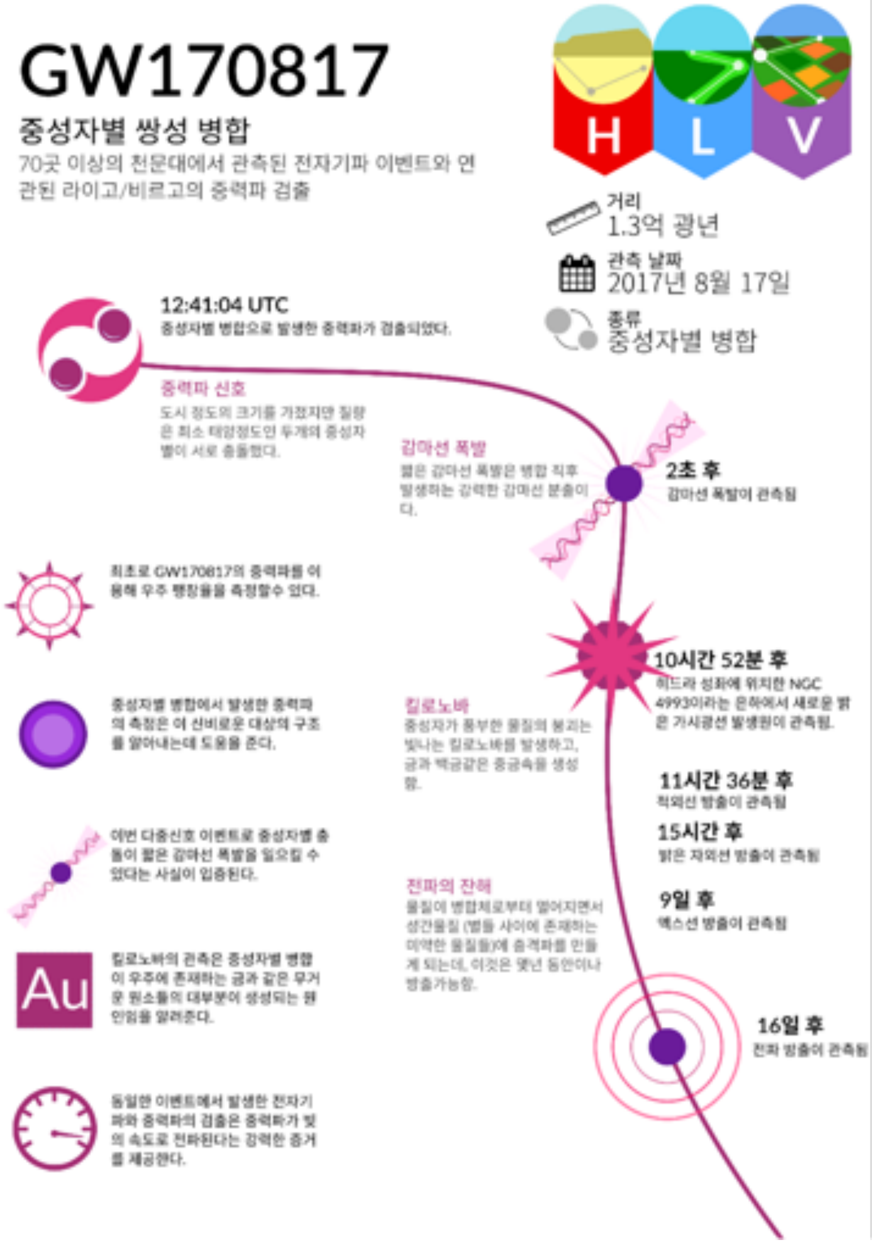

GW170817
중성자별 쌍성 병합
70곳 이상의 천문대에서 관측된 전자기파 이벤트와 연
관된 라이고/비르고의 중력파 검출
H
L
V
거리
1.3억 광년
관측 날짜
2017년 8월 17일
종류
중성자별 병합
12:41:04 UTC
중성자별 병합으로 발생한 중력파가 검출되었다.
중력파 신호
도시 정도의 크기를 가졌지만 질량
은 최소 태양정도인 두개의 중성자
별이 서로 충돌했다.
감마선 폭발
짧은 감마선 폭발은 병합 직후
발생하는 강력한 감마선 분출이
다.
2초 후
감마선 폭발이 관측됨
최초로 GW170817의 중력파를 이
용해 우주 팽창율을 측정할수 있다.
10시간 52분 후
히드라 성좌에 위치한 NGC
4993이라는 은하에서 새로운 밝
은 가시광선 발생원이 관측됨.
중성자별 병합에서 발생한 중력파
의 측정은 이 신비로운 대상의 구조
를 알아내는데 도움을 준다.
킬로노바
중성자가 풍부한 물질의 붕괴는
빛나는 킬로노바를 발생하고,
금과 백금같은 중금속을 생성
함.
11시간 36분 후
적외선 방출이 관측됨
15시간 후
밝은 자외선 방출이 관측됨
이번 다중신호 이벤트로 중성자별 충
돌이 짧은 감마선 폭발을 일으킬 수
있다는 사실이 입증된다.
전파의 잔해
물질이 병합체로부터 멀어지면서
성간물질 (별들 사이에 존재하는
미약한 물질들)에 충격파를 만들
게 되는데, 이것은 몇년 동안이나
방출가능함.
9일 후
엑스선 방출이 관측됨
Au
킬로노바의 관측은 중성자별 병합
이 우주에 존재하는 금과 같은 무거
운 원소들의 대부분이 생성되는 원
인임을 알려준다.
16일 후
전파 방출이 관측됨
동일한 이벤트에서 발생한 전자기
파와 중력파의 검출은 중력파가 빛
의 속도로 전파된다는 강력한 증거
를 제공한다.

DATA RELEASE POLICY

- O1 data are public since end of January 2018 (24 months after end of run)
- O2 data will be public end of February 2019 (24 months after end of run)

- Future bulk releases are planned to be (no later than) **18 months after the end of a 6-month data acquisition period**
  e.g., if O3 starts in April 2019, the first planned bulk data release would be **April 2021**

O3a Summary

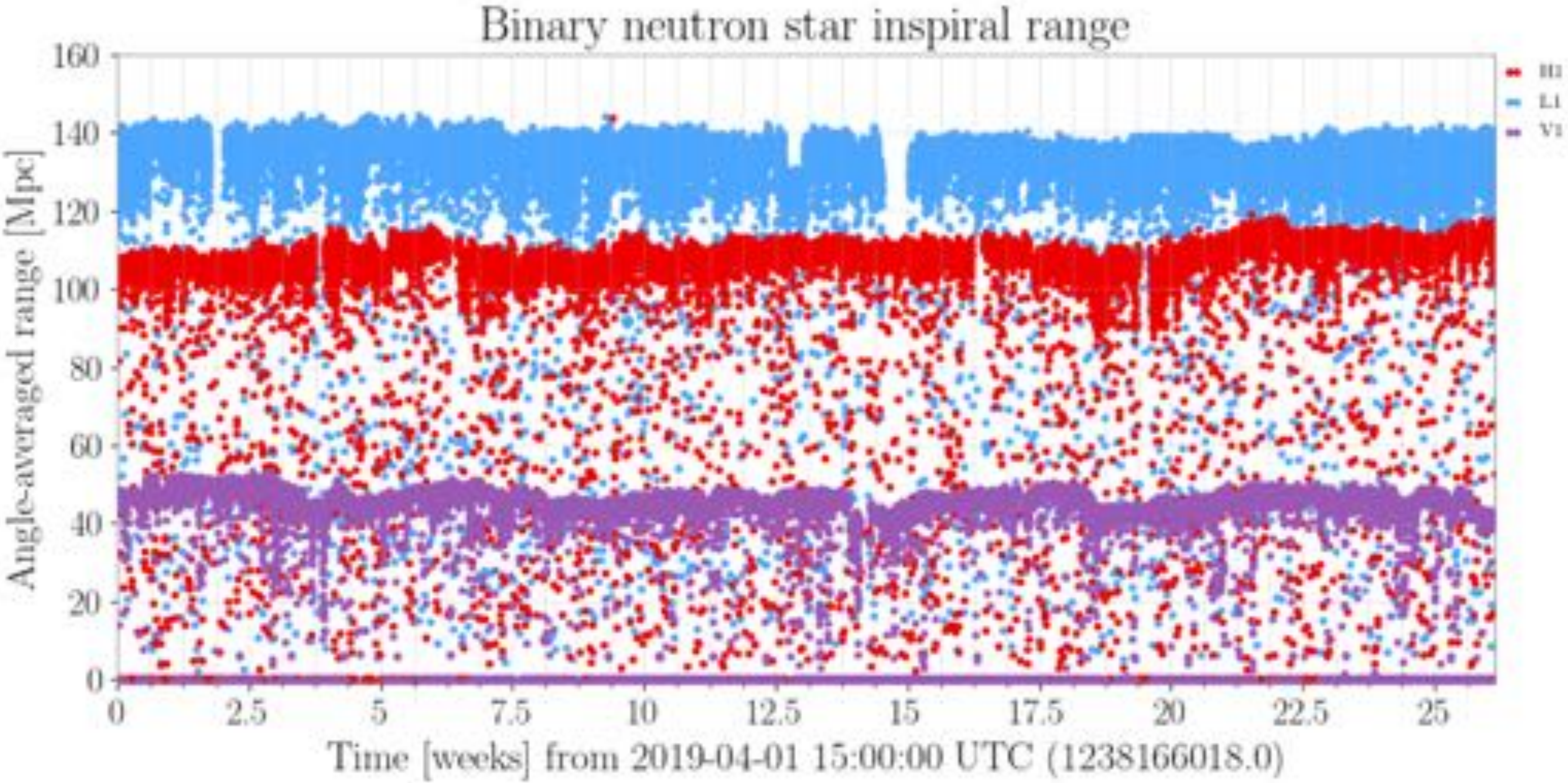

Binary neutron star inspiral range
Angle-averaged range [Mpc]
160
140
120
100
80
60
40
20
0
H1
L1
V1
0
2.5
5
7.5
10
12.5
15
17.5
20
22.5
25
Time [weeks] from 2019-04-01 15:00:00 UTC (1238166018.0)

O3 is on-going

- https://gracedb.ligo.org/latest/

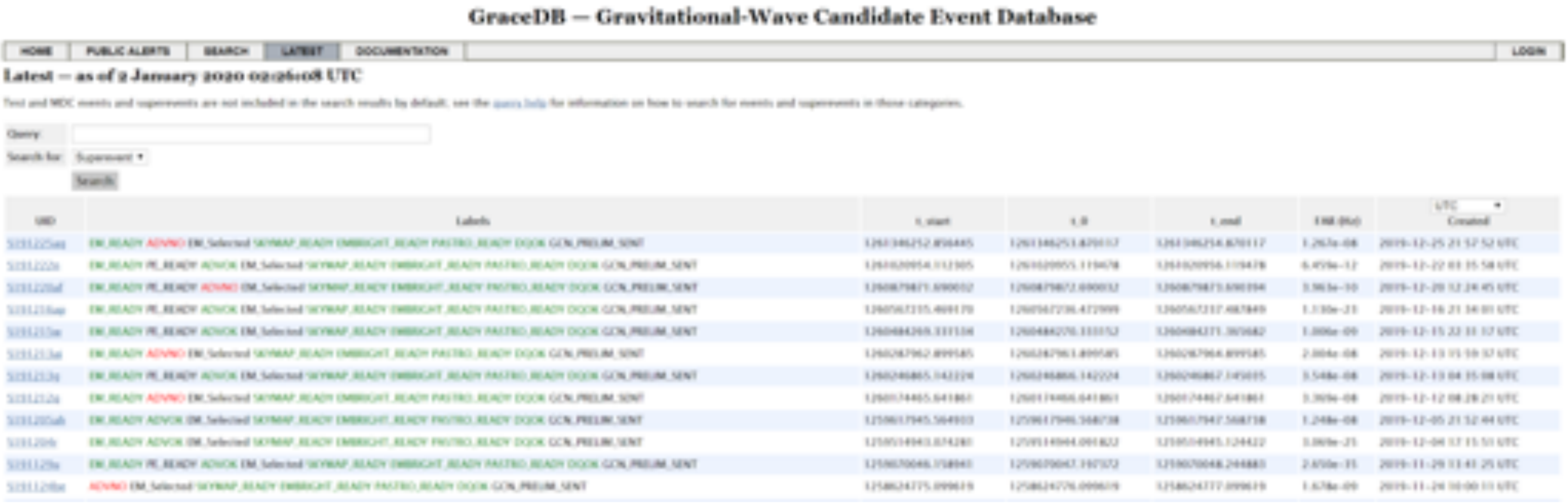

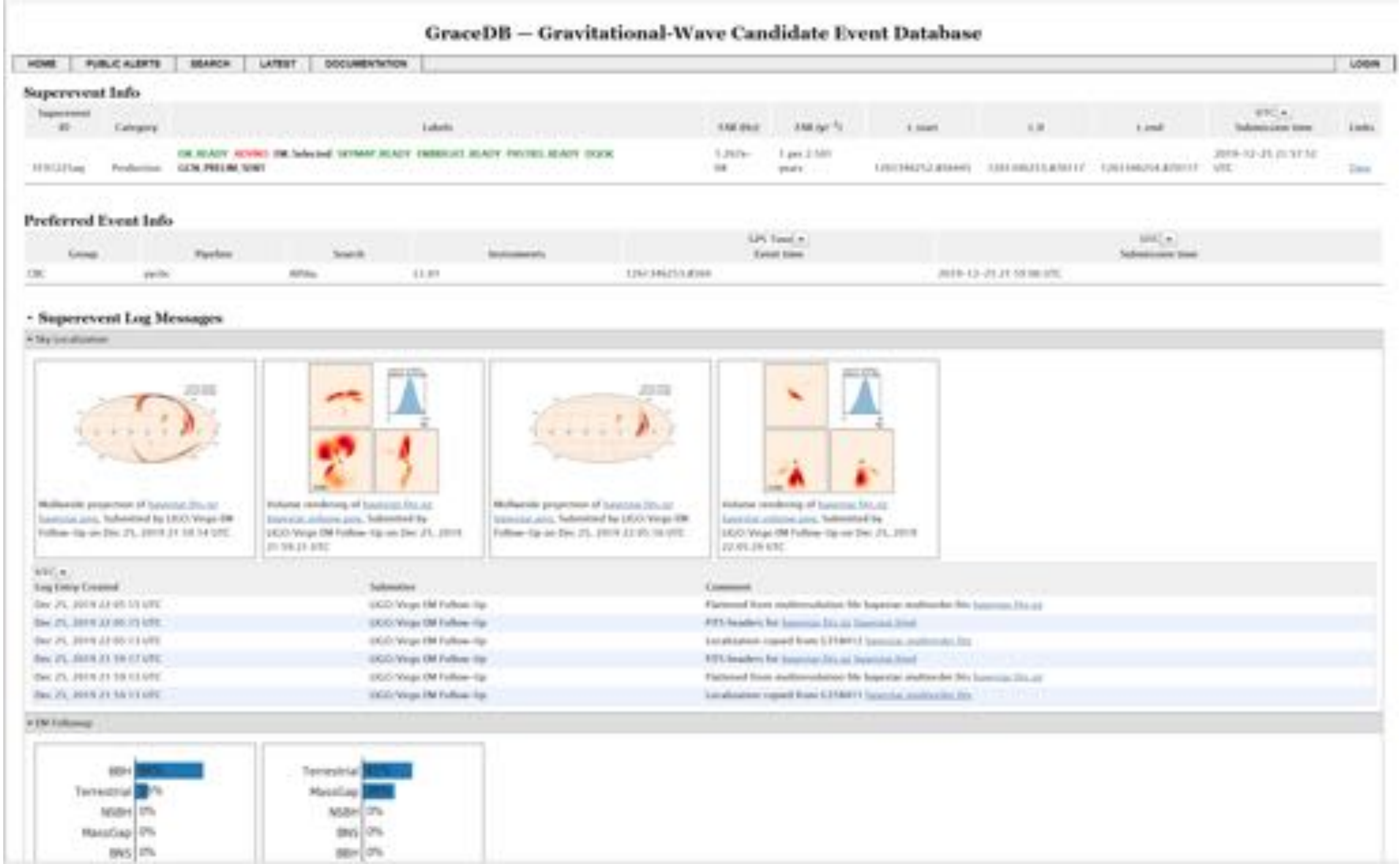
GraceDB — Gravitational-Wave Candidate Event Database
HOME
PUBLIC ALERTS
SEARCH
LATEST
DOCUMENTATION
LOGIN
Superevent Info
Preferred Event Info
Superevent Log Messages
BBH
Terrestrial
NSBH
MassGap
BNS

Gravitational Wave Open Science Center

Data ▾ Software ▾ Online Status ▾ About GWOSC ▾

Gravitational Wave Events and Catalogs

Event Portal

The **Event Portal** provides access to gravitational-wave events and catalogs.

GWTC-1

Gravitational-Wave Transient Catalog of Compact Binary Mergers (O1 & O2)

- **Documentation:** Notes
- **Strain Data:** Confident detections | Marginal Triggers
- **Auxillary Data:** PE Samples, Skymaps, and more

Older event releases

Previous event releases are also available.

https://www.gw-openscience.org/catalog/

LSC EGO VIRGO

The Gravitational Wave Spectrum

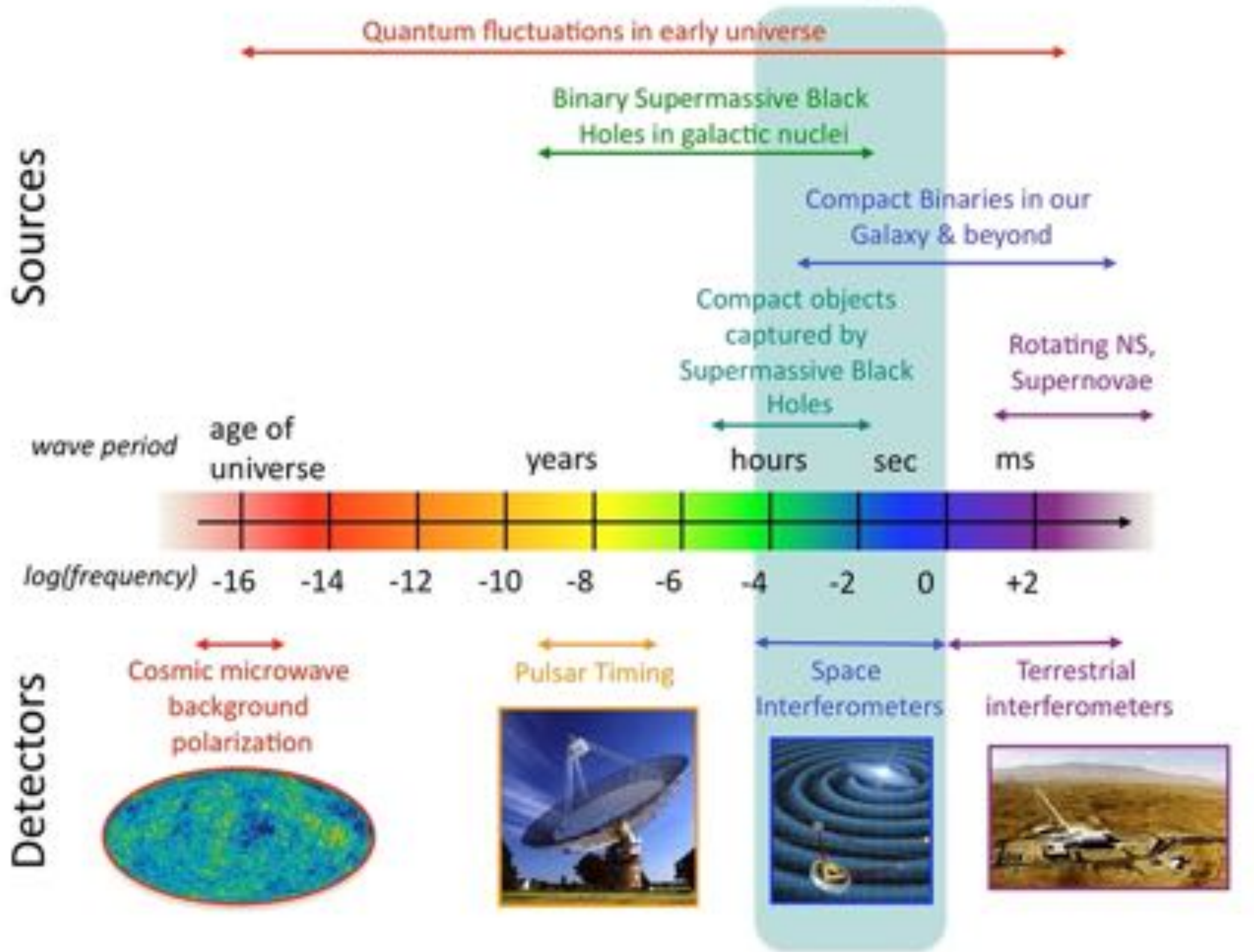

Basic principle

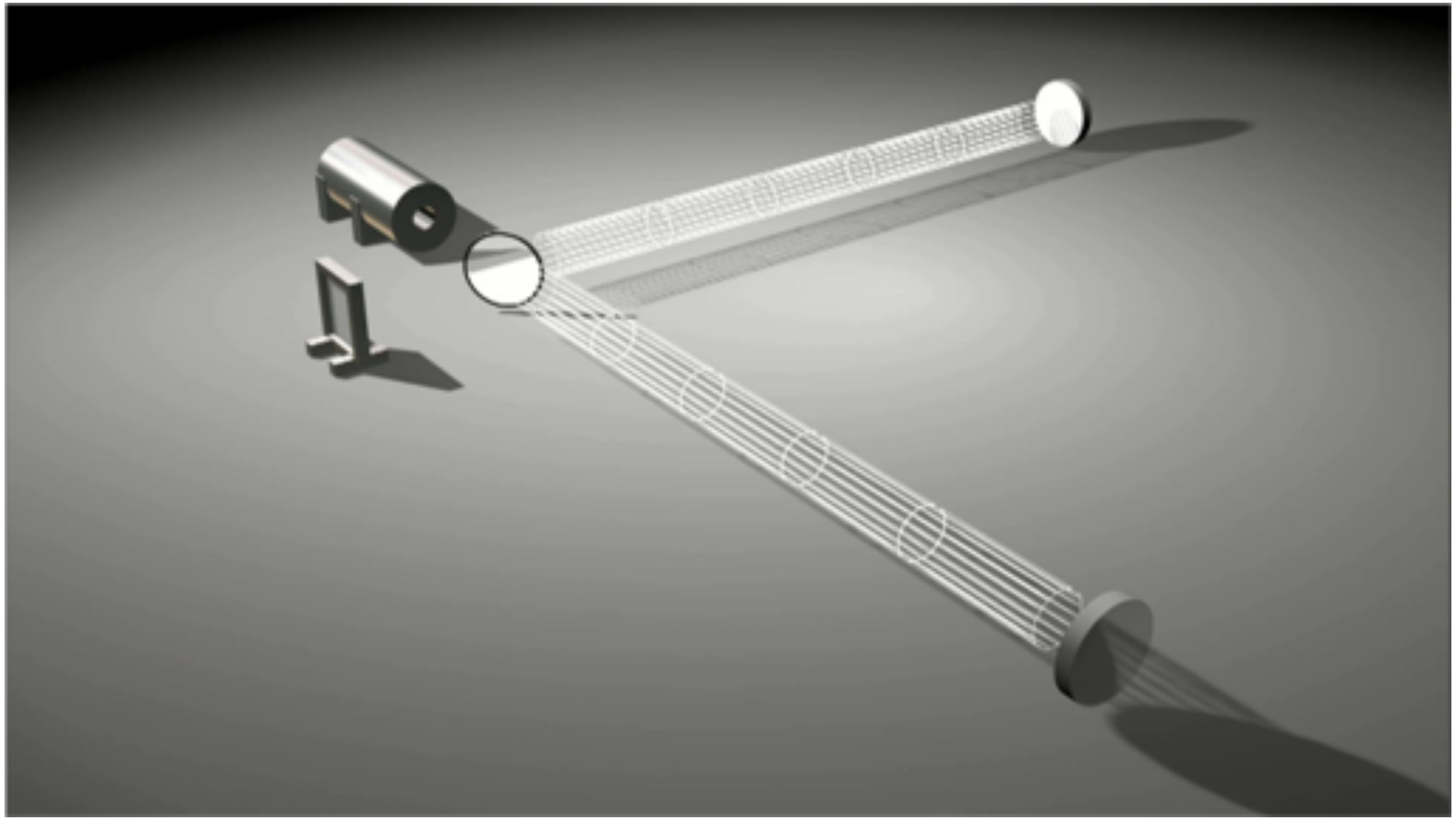

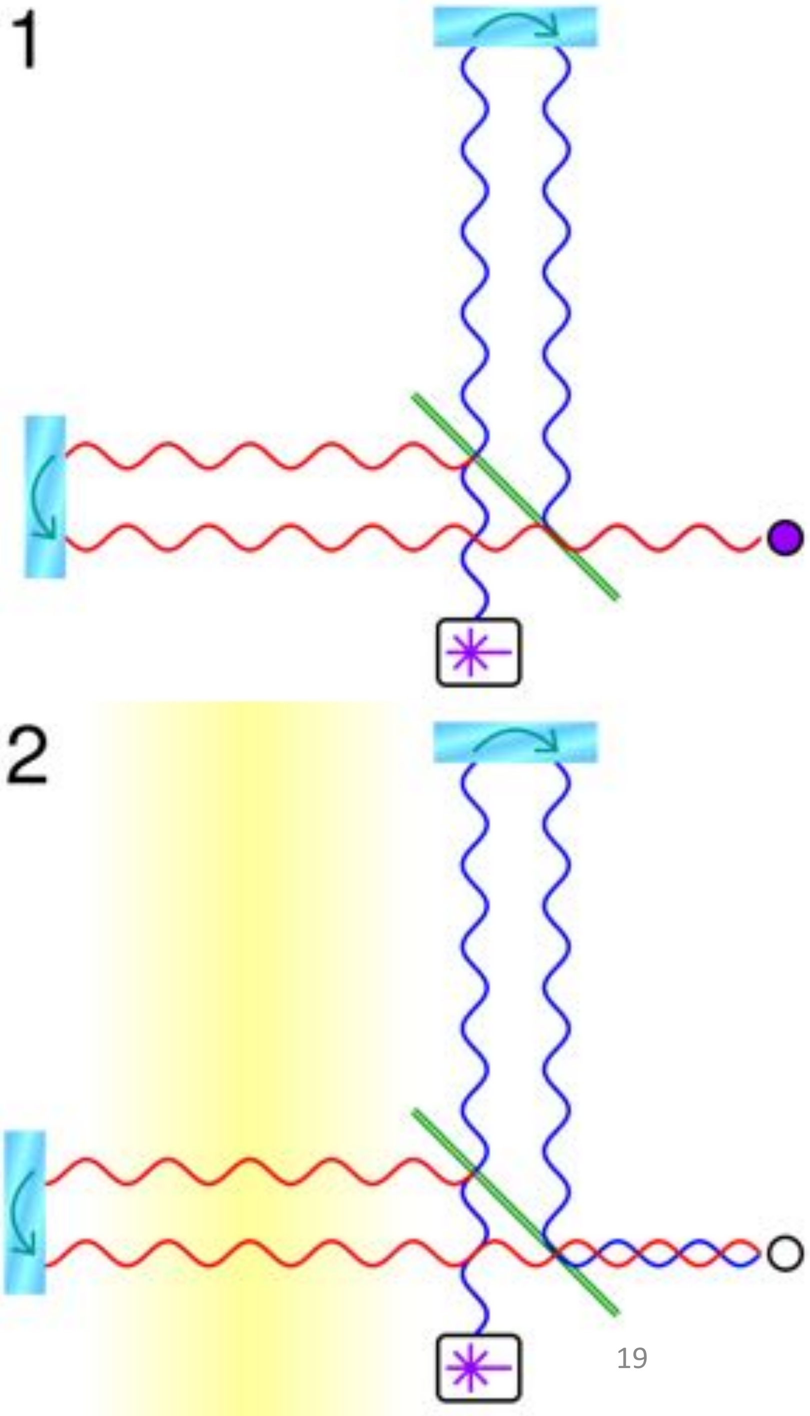

Properties of LIGO-Virgo data

Sketch S. Hild

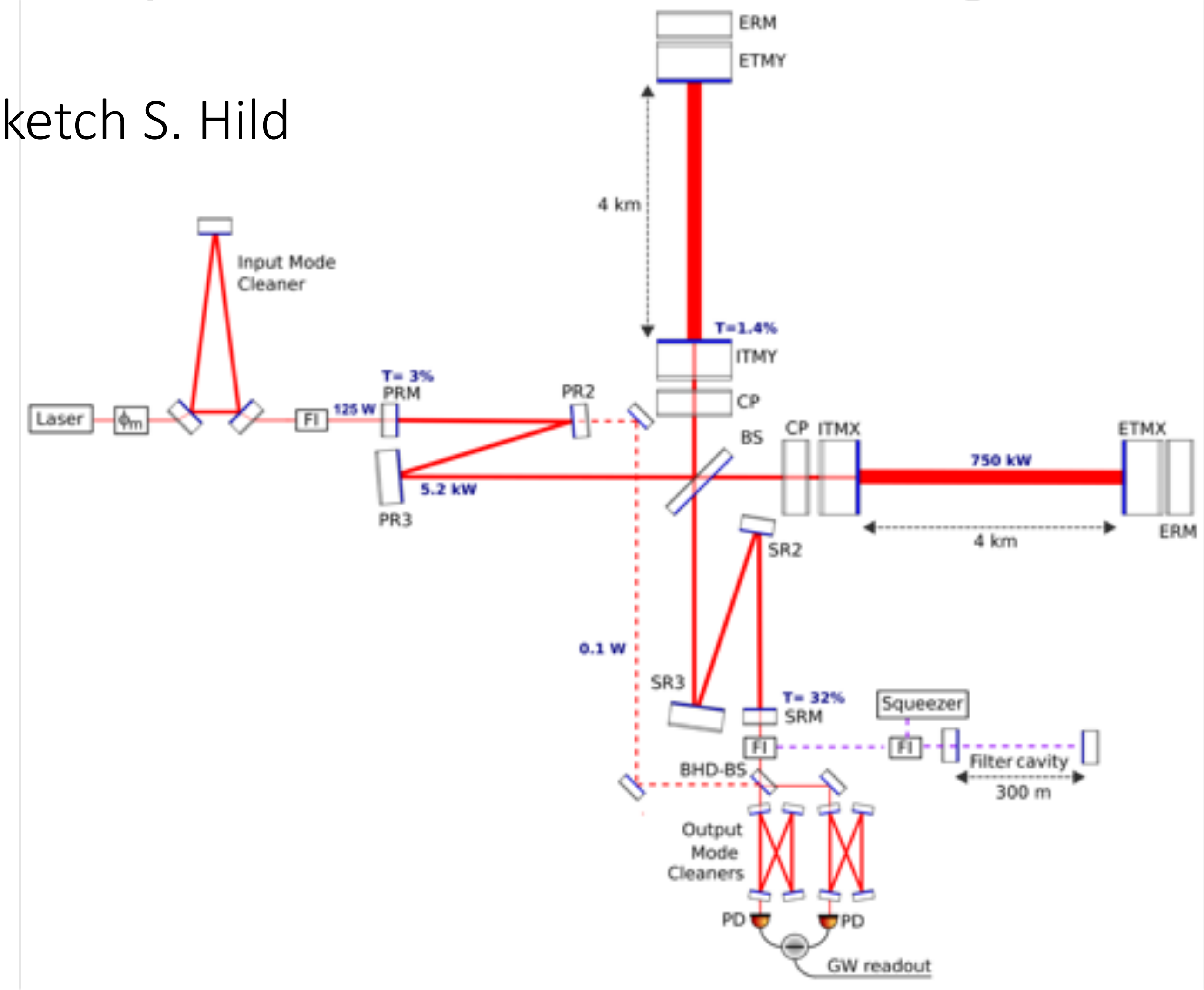

- Sampling rate
  - 16384Hz:LIGO
  - 20kHz:Virgo
  - 16384Hz:KAGRA
- Valid range
  - 10Hz~5kHz : LIGO
  - 10Hz~8kHz : Virgo
  - 10Hz~5kHz : KAGRA(?)

Basic properties of detector noise

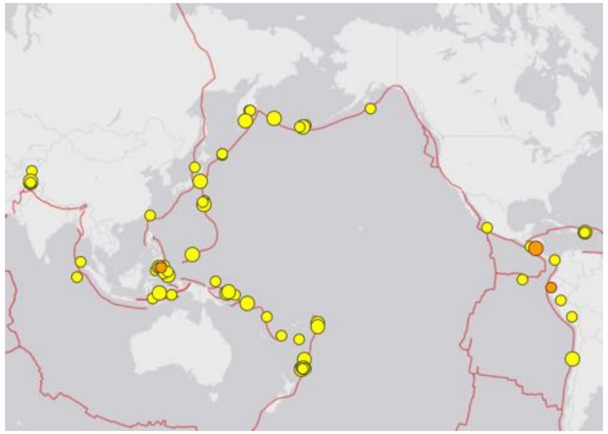

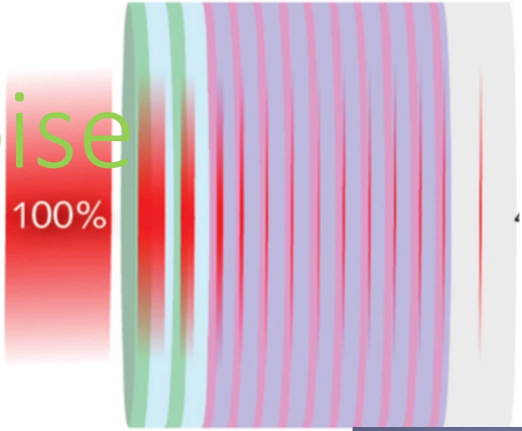

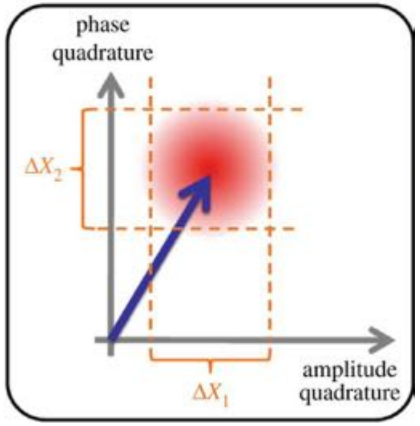

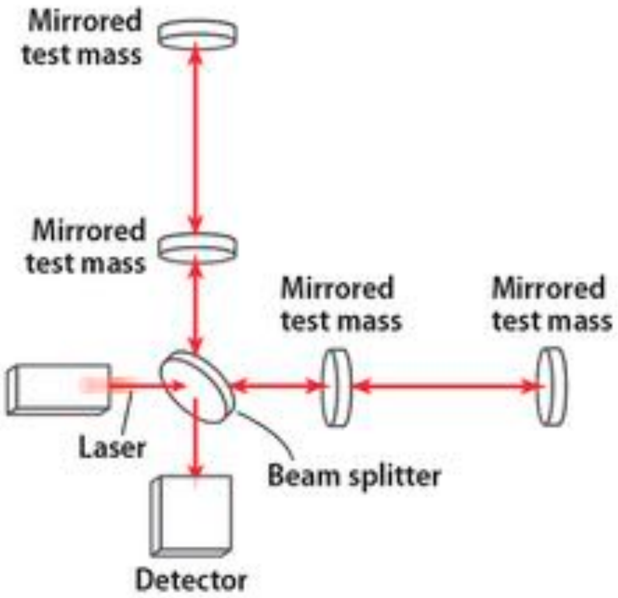

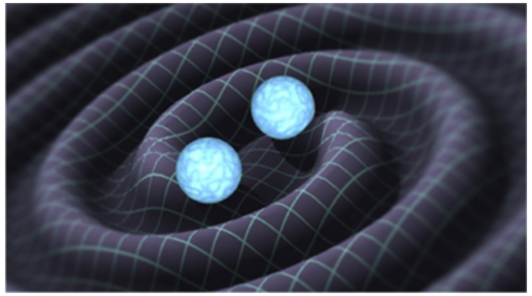

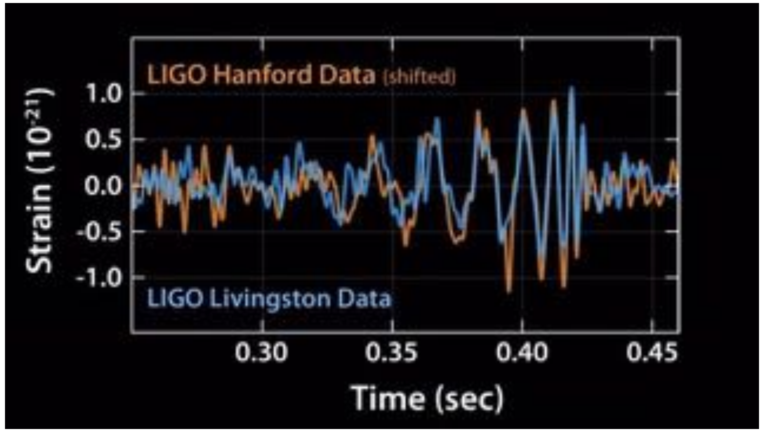

Noise budget of AdvLIGO

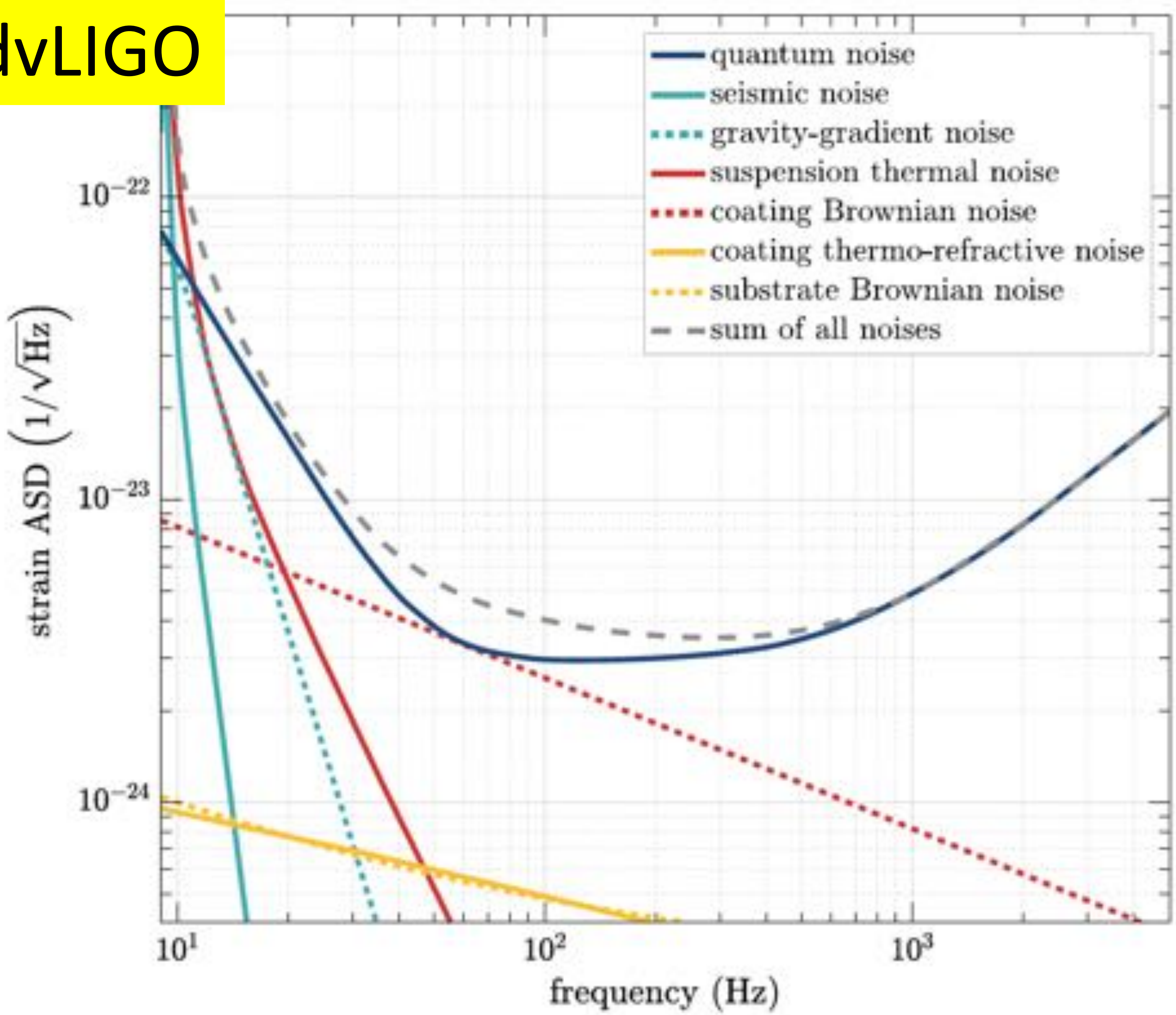

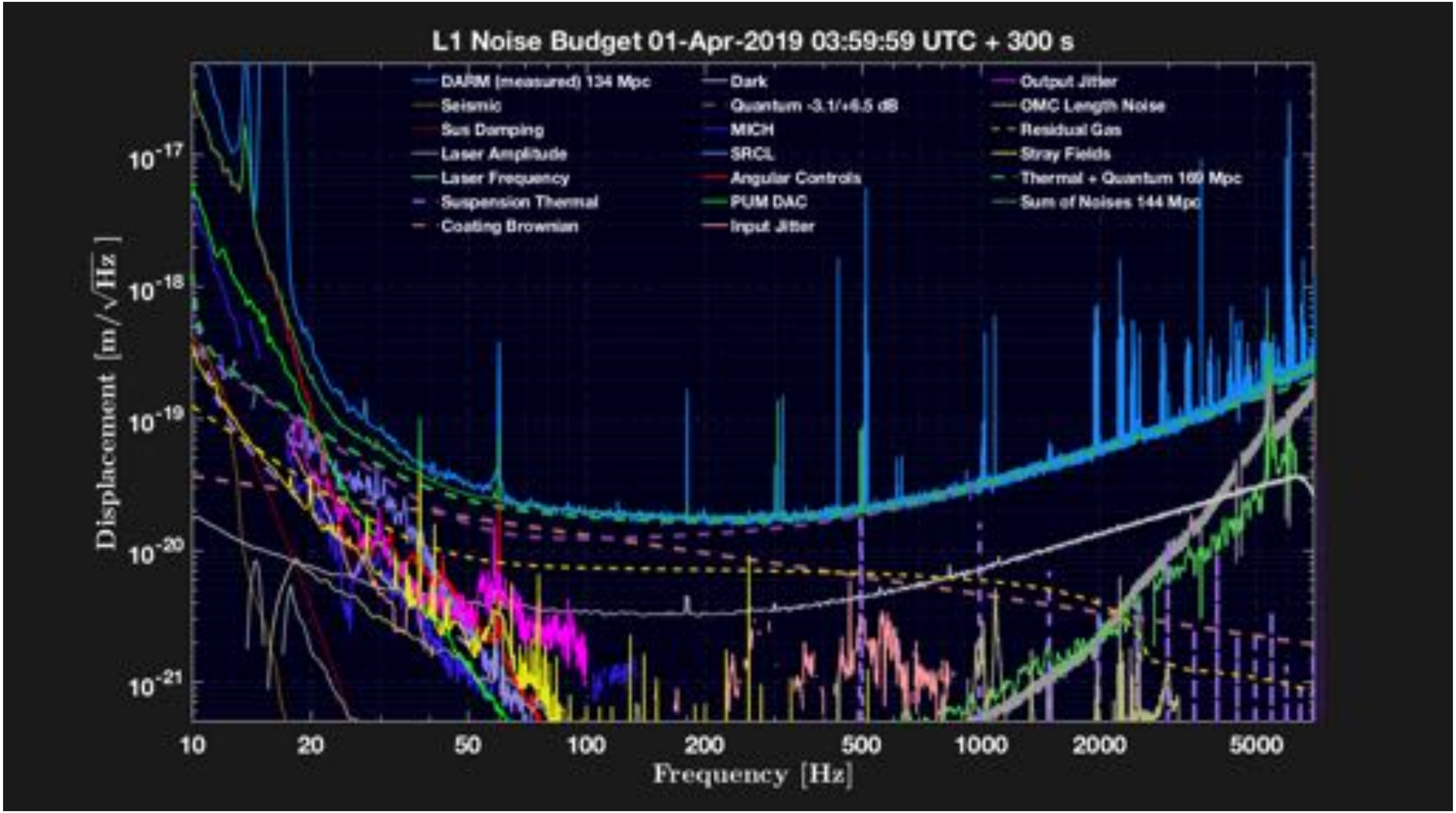
L1 Noise Budget 01-Apr-2019 03:59:59 UTC + 300 s
DARM (measured) 134 Mpc
Seismic
Sus Damping
Laser Amplitude
Laser Frequency
Suspension Thermal
Coating Brownian
Dark
Quantum -3.1/+6.5 dB
MICH
SRCL
Angular Controls
PUM DAC
Input Jitter
Output Jitter
OMC Length Noise
Residual Gas
Stray Fields
Thermal + Quantum 169 Mpc
Sum of Noises 144 Mpc
Displacement [m/√Hz]
Frequency [Hz]

Quantum Noise

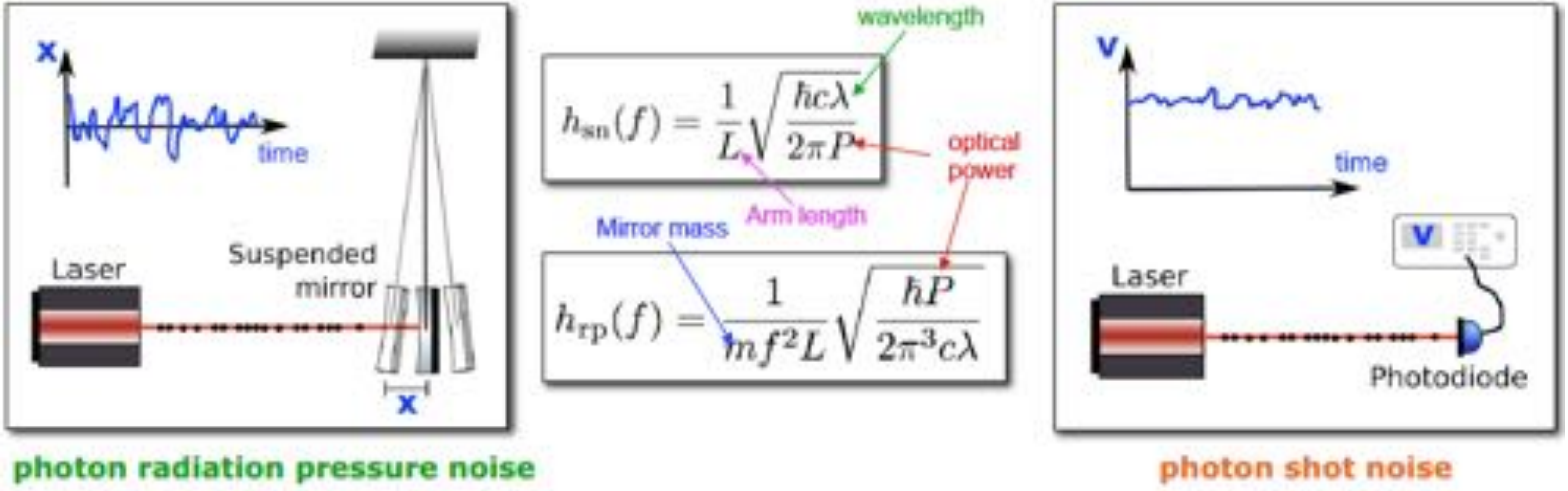

Detector Noise

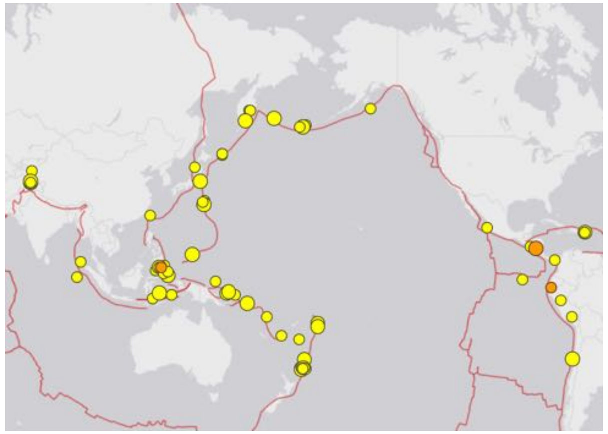

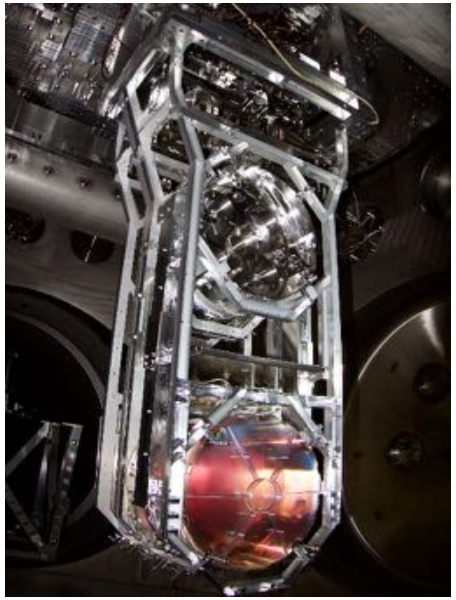

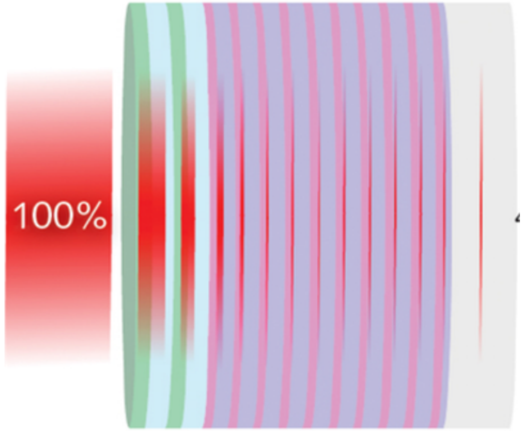

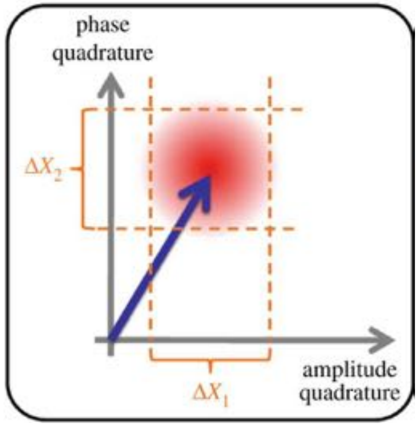

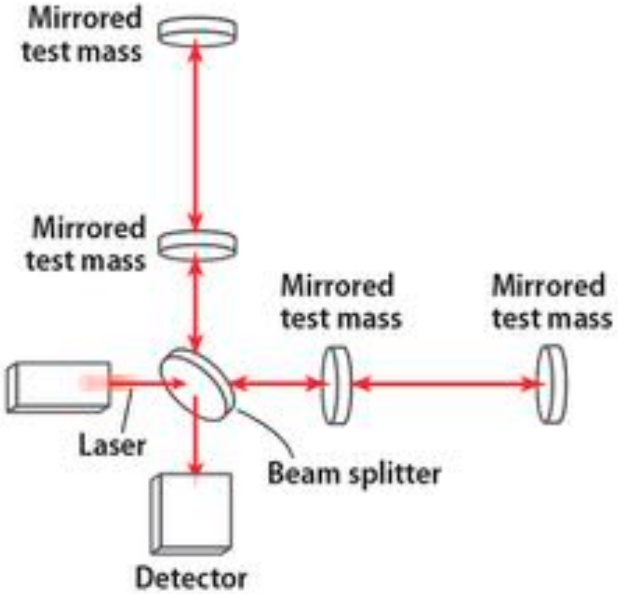

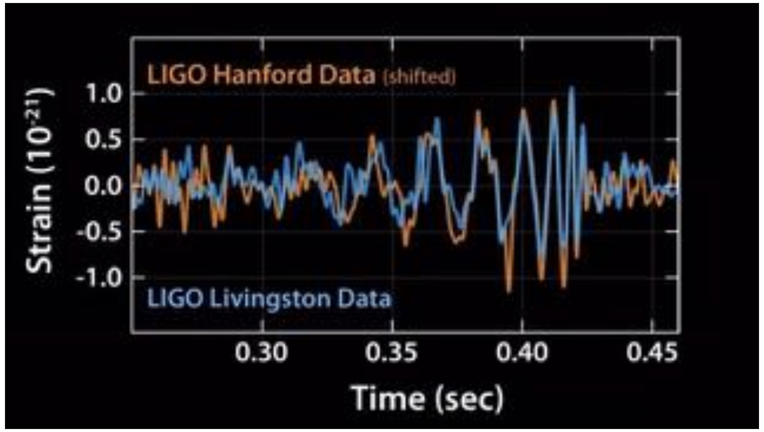

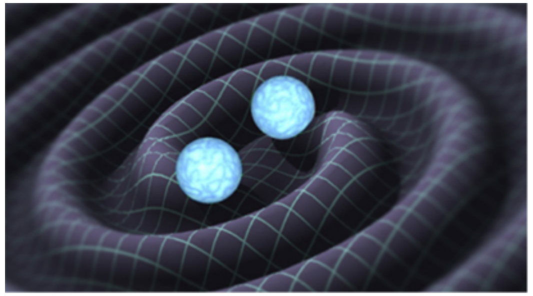

Data Analysis

$$d(t) \xrightarrow{\text{FFT}} \tilde{d}(f) \xrightarrow{\text{Whiten}} \tilde{d}_w(f) = \frac{\tilde{d}(f)}{S_n^{1/2}(f)} \xrightarrow{\text{iFFT}} d_w(t)$$

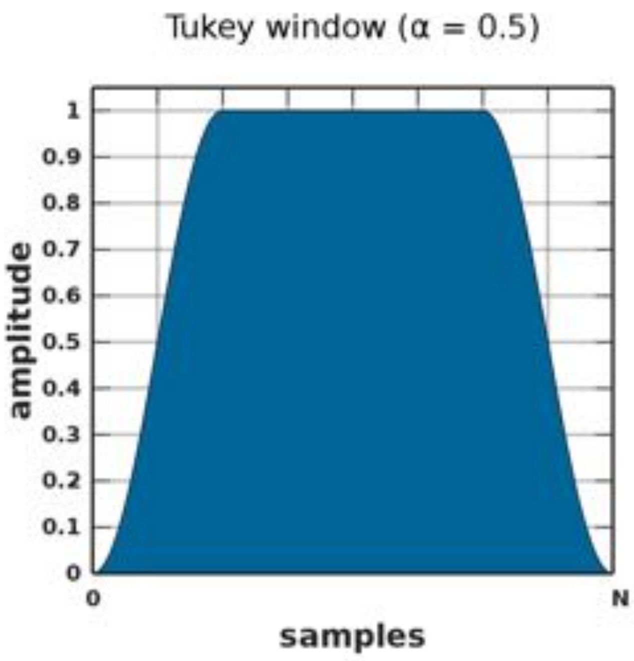

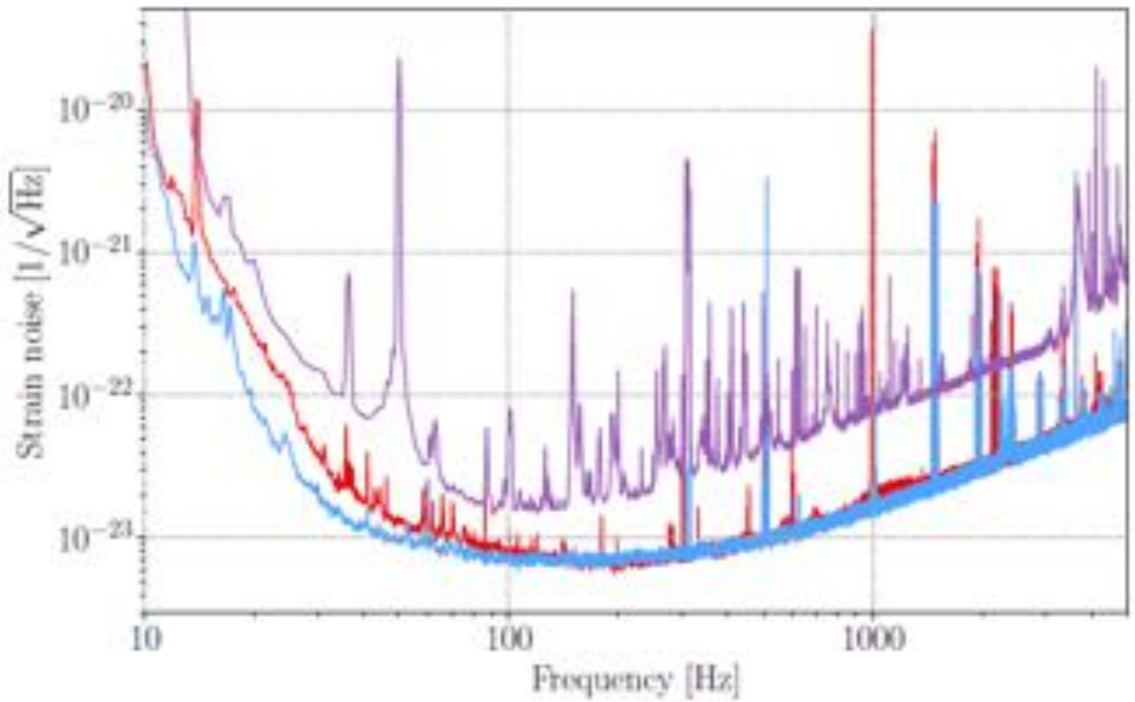

- GW150914

$$
\left.
\begin{aligned}
w[n] &= \frac{1}{2}\left[1-\cos\left(\frac{2\pi n}{\alpha L}\right)\right], && 0 \le n < \frac{\alpha L}{2} \\
w[n] &= 1, && \frac{\alpha L}{2} \le n \le \frac{N}{2} \\
w[N-n] &= w[n], && 0 \le n \le \frac{N}{2}
\end{aligned}
\right\}
$$

Tukey window (α = 0.5)

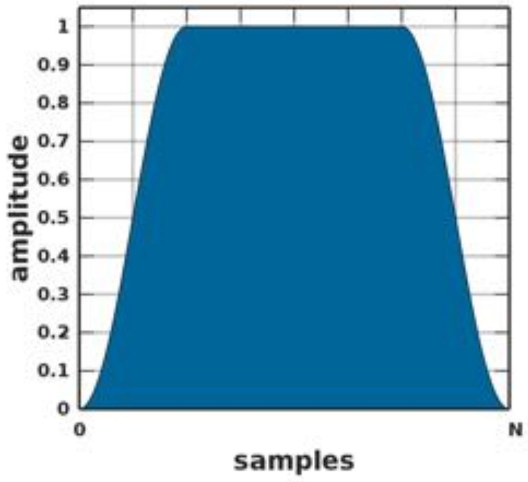

Fourier transform

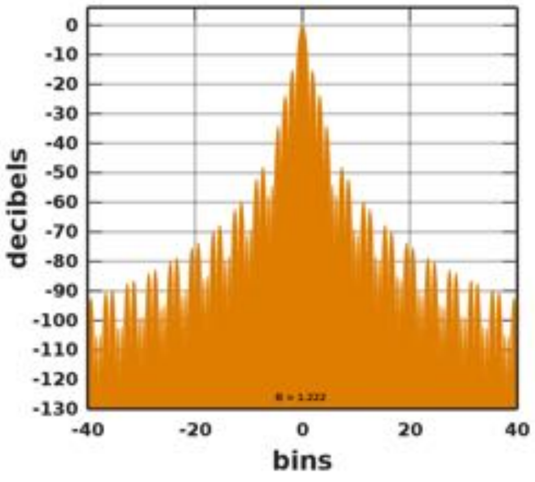

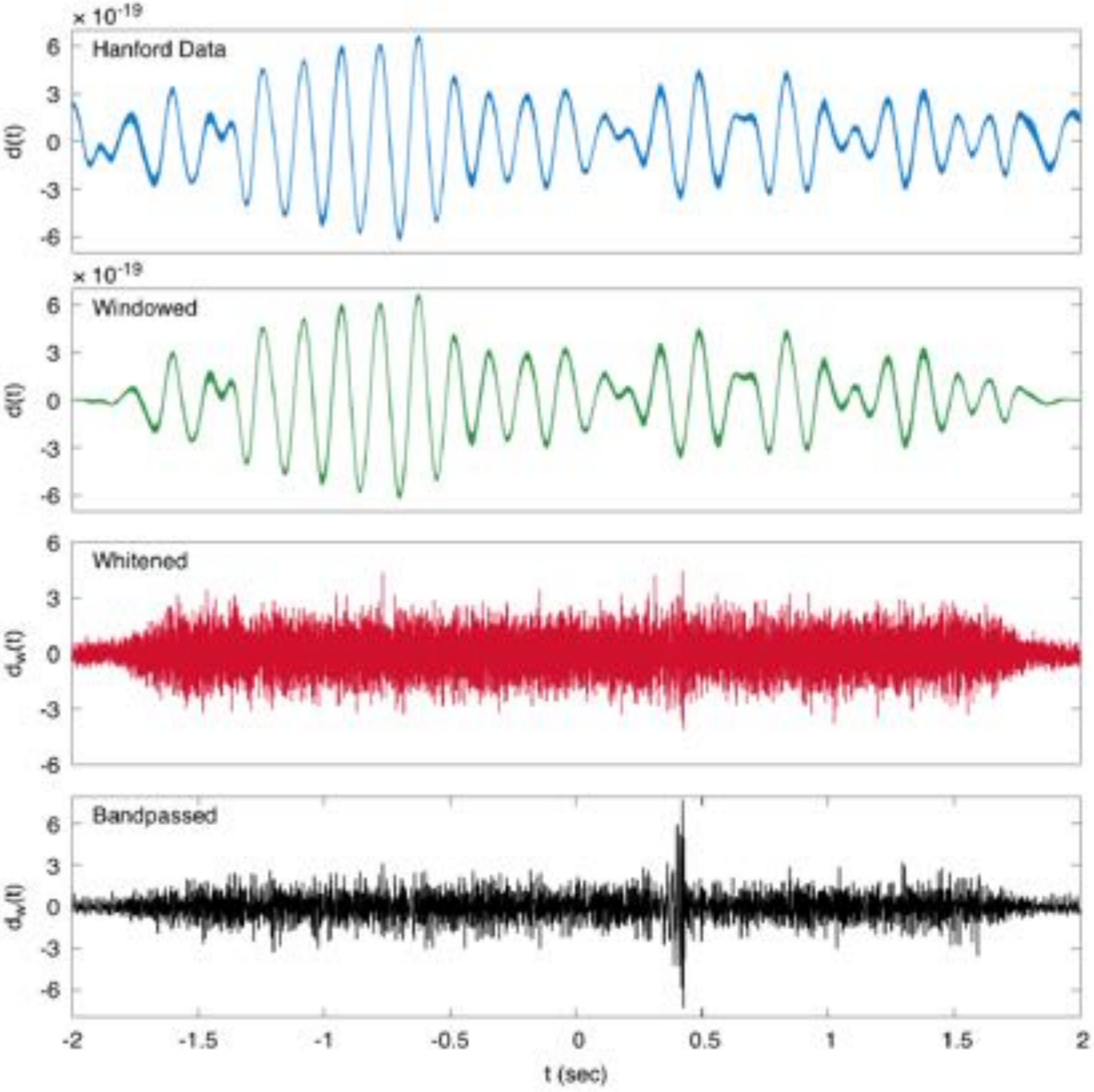

Spectrum

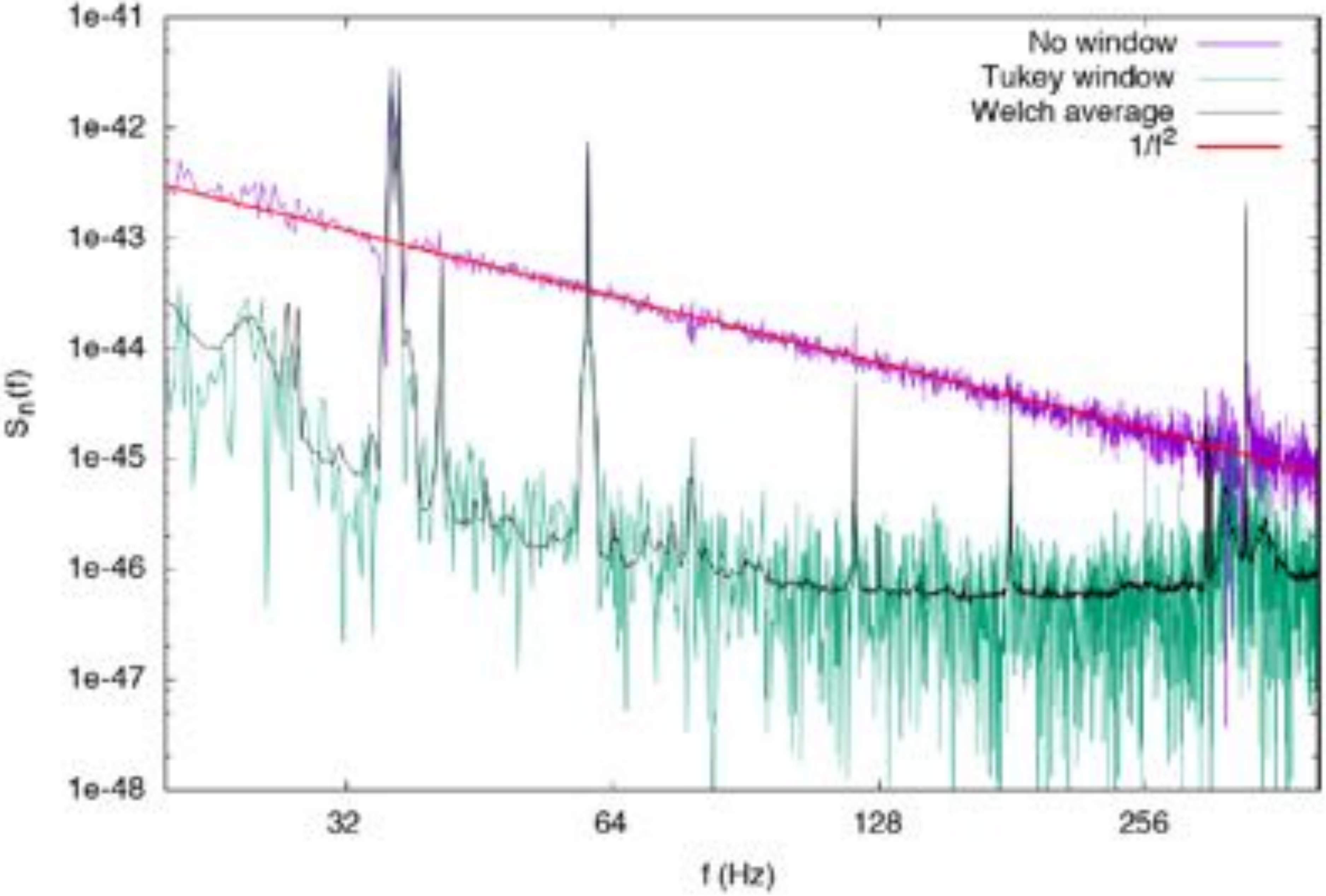

No window
Tukey window
Welch average
$1/f^2$
1e-41
1e-42
1e-43
1e-44
1e-45
1e-46
1e-47
1e-48
$S_n(f)$
32
64
128
256
f (Hz)

h(t) graph

KAGALI h(t) data
Window function : Tukey with 5% padding
Strain data : L-L1_LOSC_16_V1-1126256640-4096.gwf
Channel : L1:GWOSC-16KHZ_R1_STRAIN
Trigger time : 1126259462
Segment length : 16s

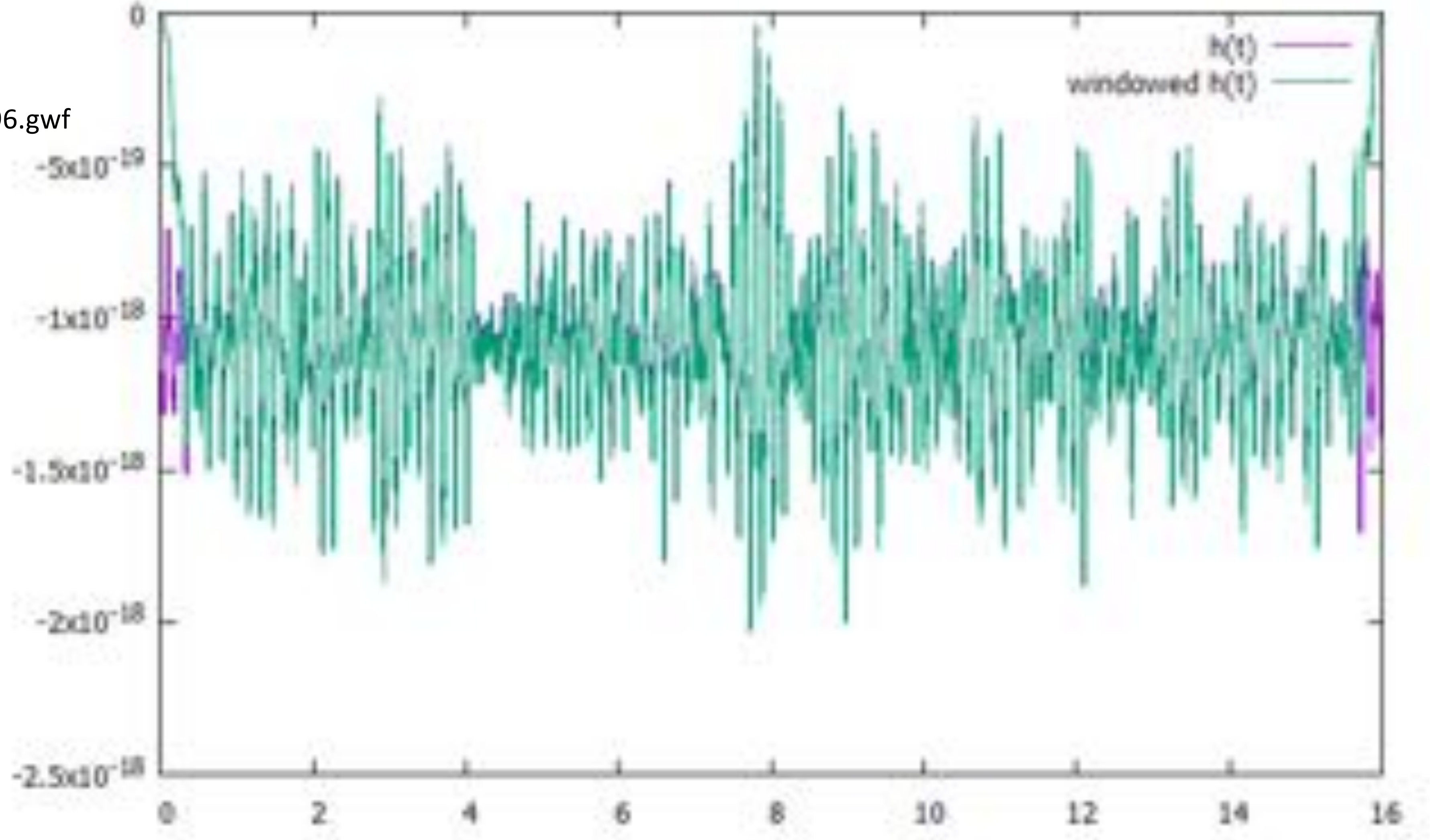

Spectrum

LALSuite and KAGALI h(f) comparison

Window function : Tukey with 0.4 sec padding
Strain data : L-L1_LOSC_16_V1-1126256640-4096.gwf
Channel : L1:GWOSC-16KHZ_R1_STRAIN
Trigger time : 1126259462
Segment length : 16s

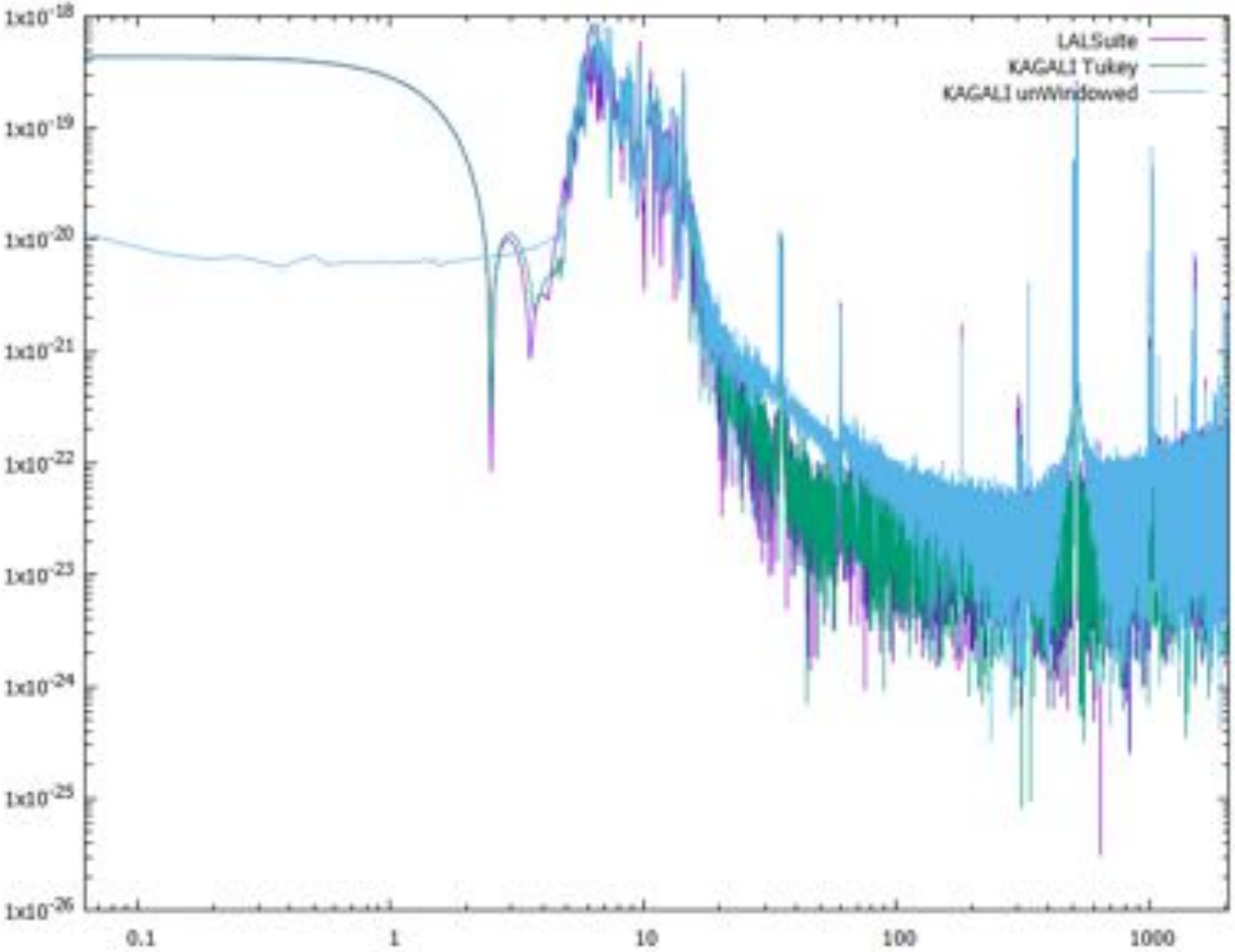

Phase

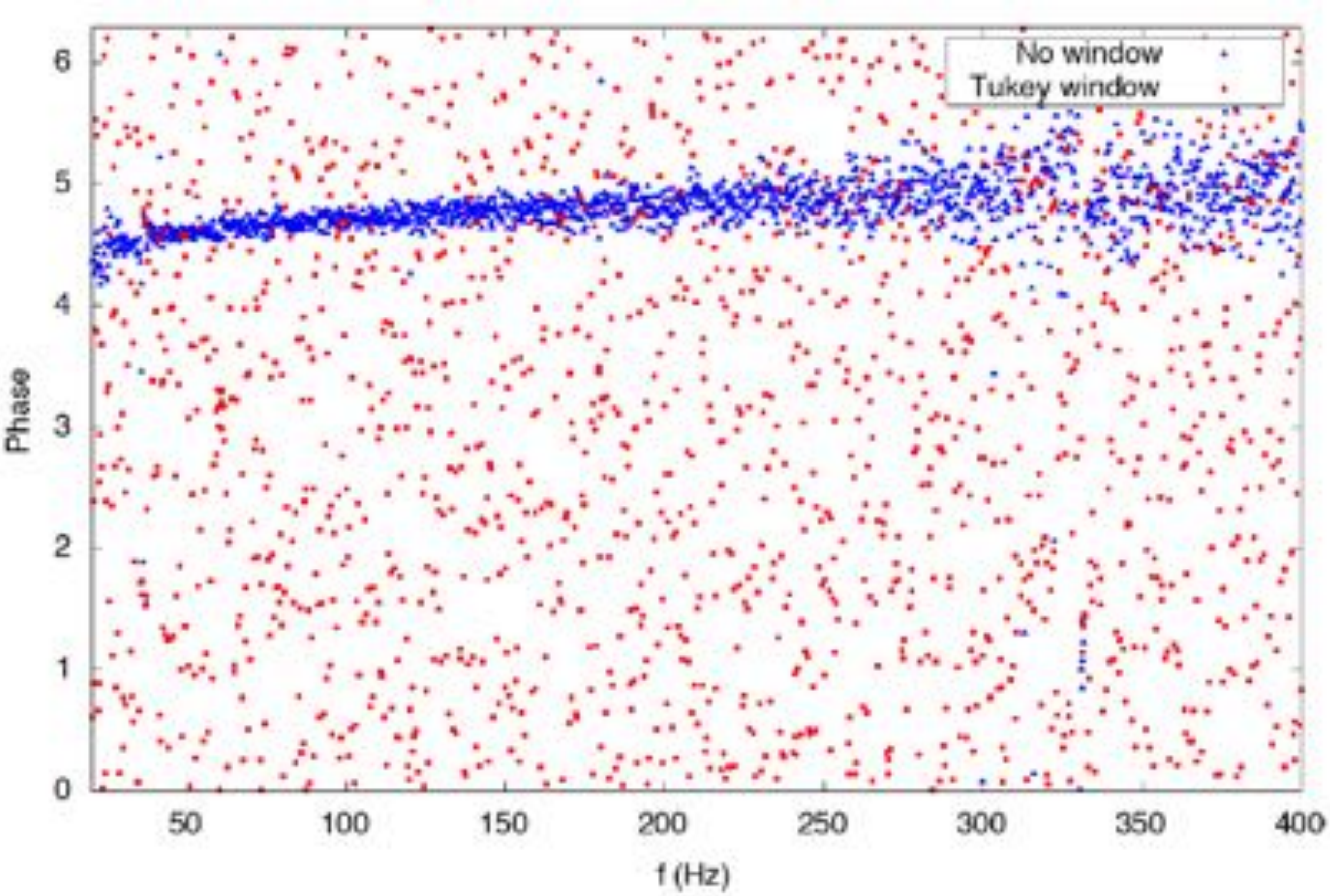

No window
Tukey window
Phase
6
5
4
3
2
1
0
50
100
150
200
250
300
350
400
f (Hz)

LALInferenceReadData.c

- LALInferenceReadData()
  - Read data file or generate fake data
  - Read PSD data file or generate from strain data
  - Resample as required sample rate
  - Windowing the time data
  - Generate frequency domain data using FFT
  - Generate whiten data in frequency and time

$$d(t) \xrightarrow{\text{FFT}} \tilde{d}(f) \xrightarrow{\text{Whiten}} \tilde{d}_w(f) = \frac{\tilde{d}(f)}{S_n^{1/2}(f)} \xrightarrow{\text{iFFT}} d_w(t)$$

PSD Estimation

- Welch average: XLALREAL8AverageSpectrumWelch()
- Median selection: XLALREAL8AverageSpectrumMedian()

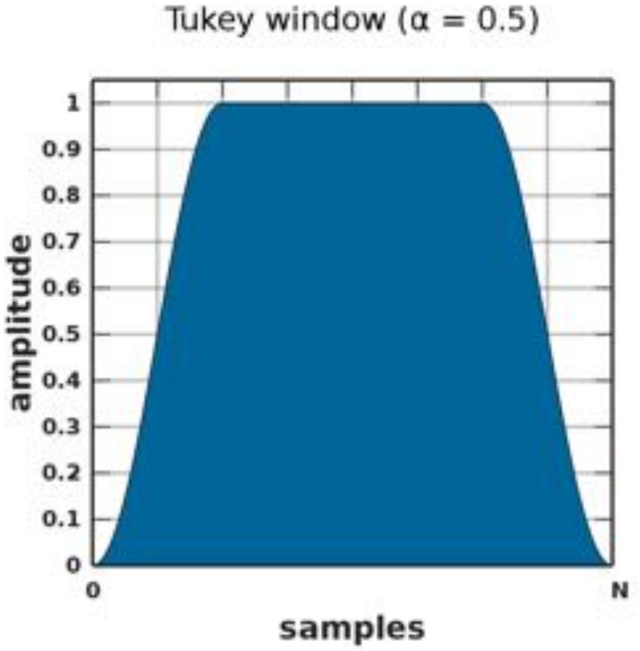

Time relations

- --trigtime : This option specifies the trigger time at geocenter, this time is same as injection time in injection table
- ifo->epoch : this time is segment start time

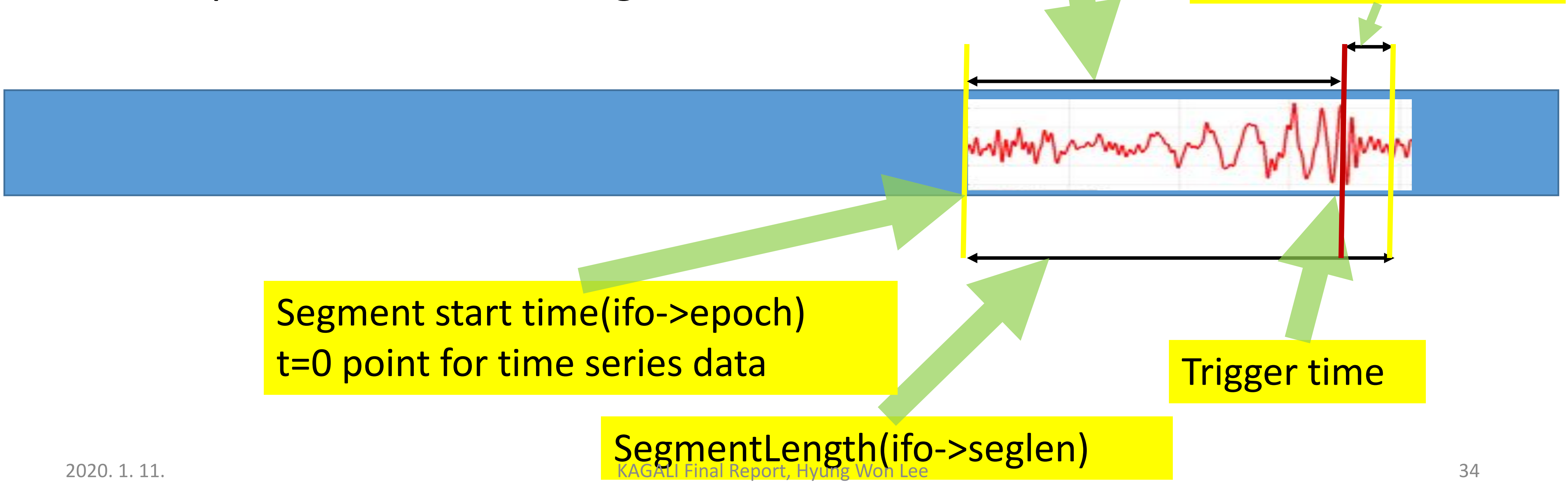

Timedelay

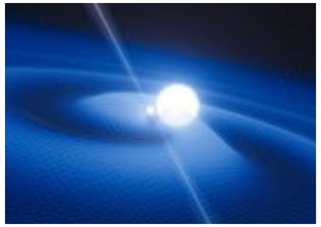

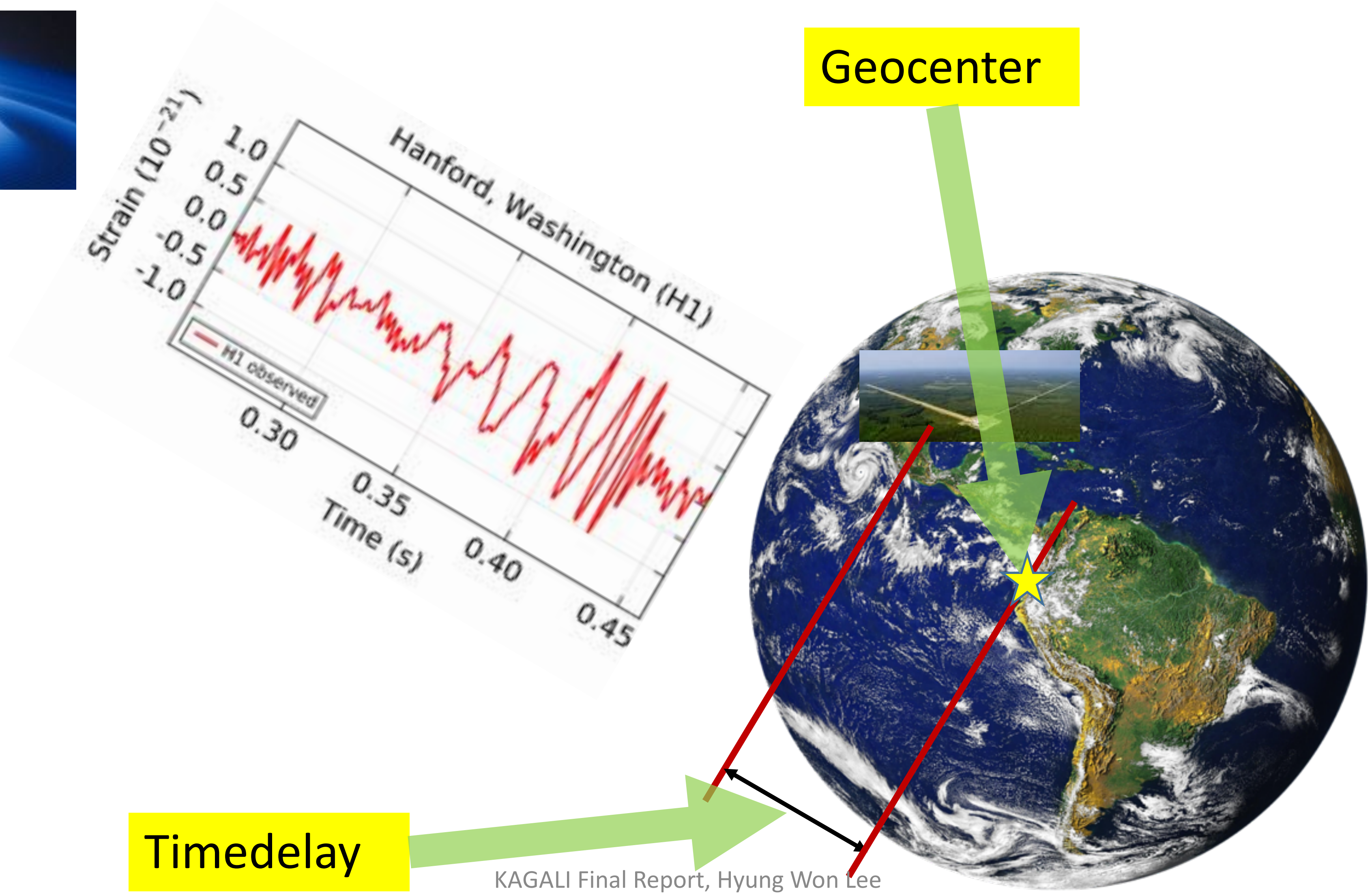
Hanford, Washington (H1)
Strain (10^-21)
1.0
0.5
0.0
-0.5
-1.0
H1 observed
0.30
0.35
0.40
0.45
Time (s)
Geocenter
Timedelay

Time-frequency analysis and stationary

- Long-term
- Short-term: glitches
- AC lines

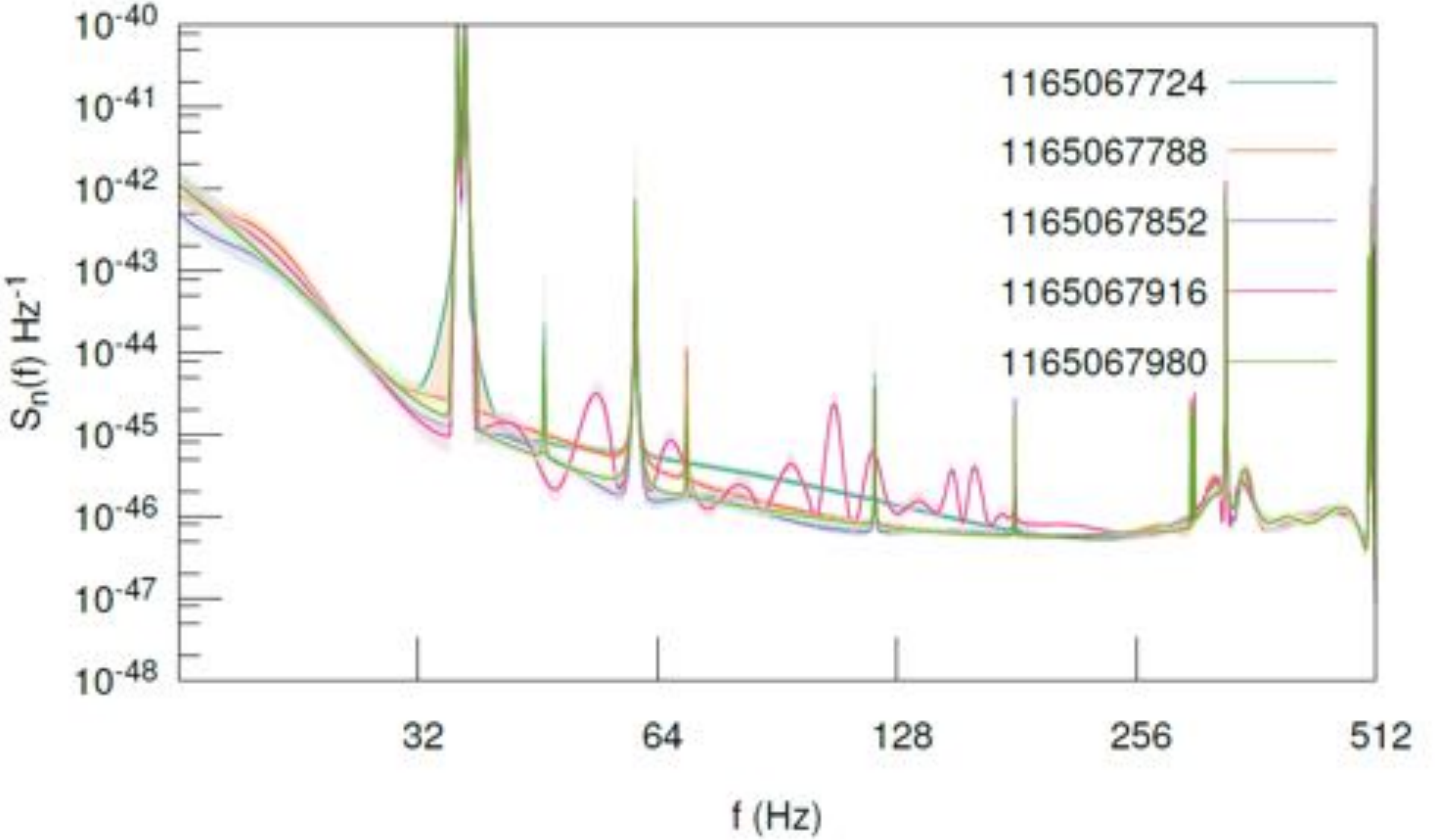

Stationarity test

- Continuous Wavelet transform(scalogram)

GPS 1165067917

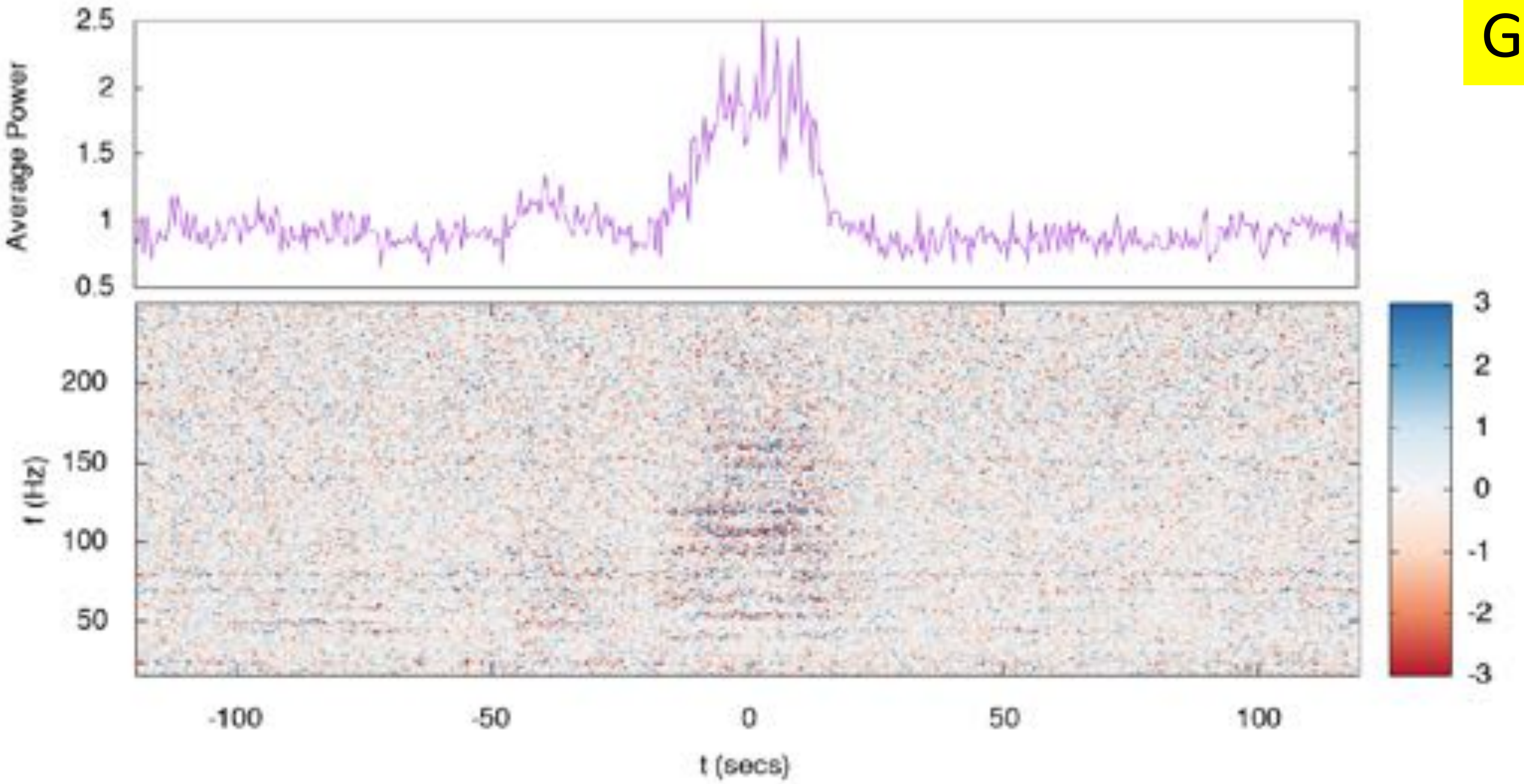

Wilson-Hilferty transfrom

- Transform Chi-square of many degree of freedom to standard one

$$W(Y) = \frac{\left(\frac{Y}{n}\right)^{1/3} - \left(1 - \left(\frac{1}{9}\right)\left(\frac{2}{n}\right)\right)}{\sqrt{\left(\frac{1}{9}\right)\left(\frac{2}{n}\right)}}$$

Wilson-Hilferty transform

GPS 1186741733
p-value: 0.74

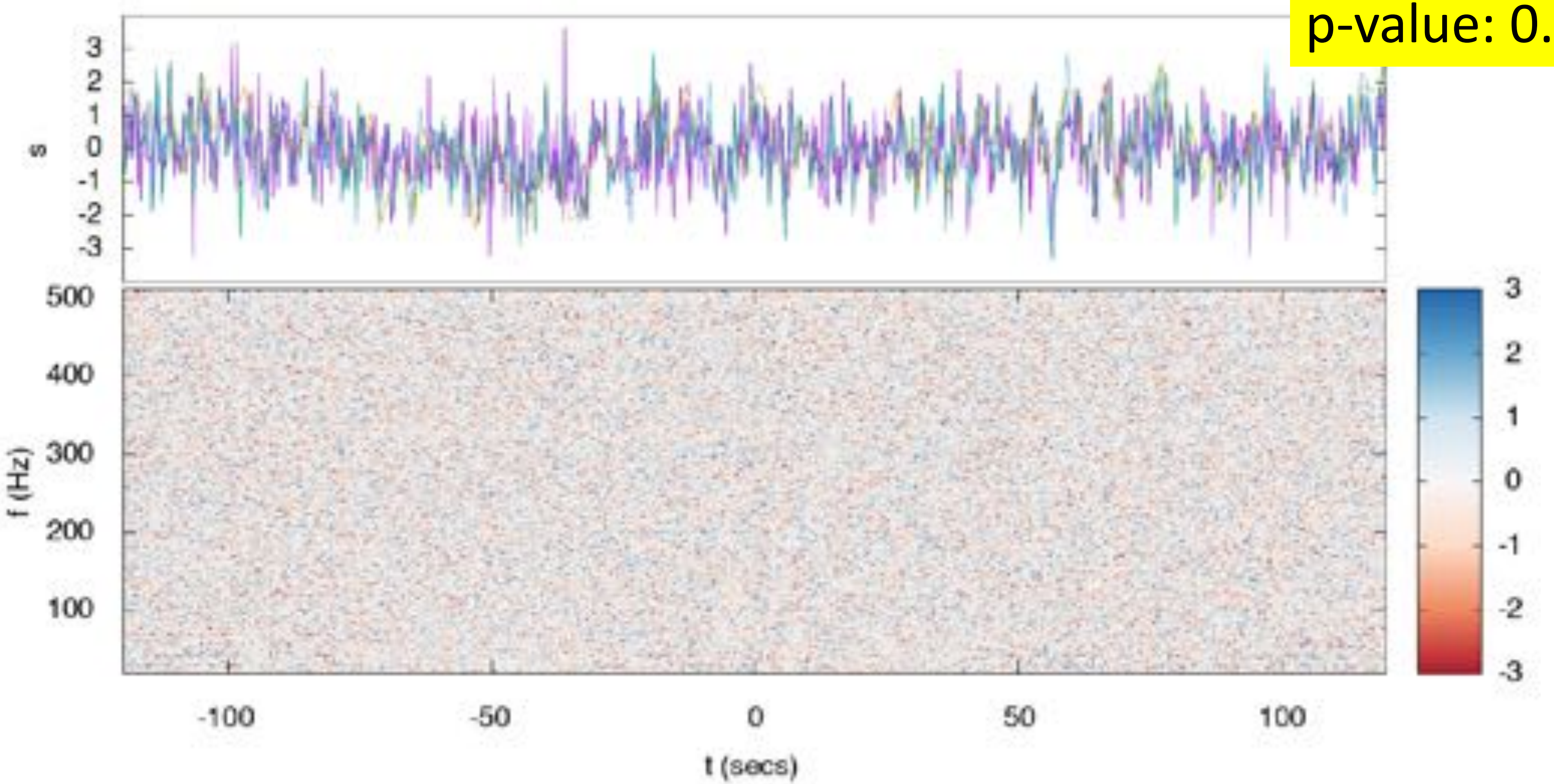

Wilson-Hilferty transform

GPS 1166358283
p-value: 2.6×10^{-6}

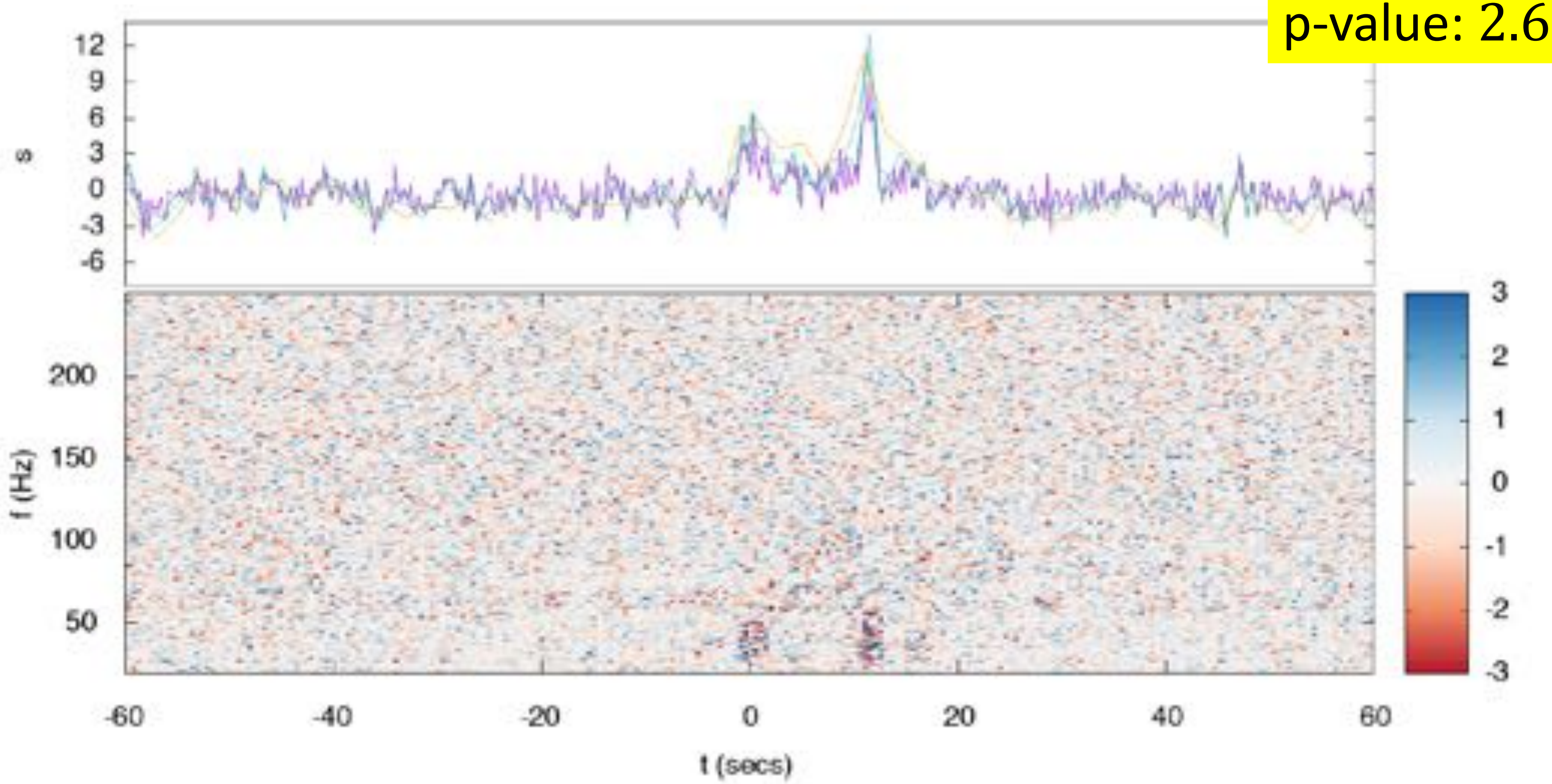

Generation of h(t)

$$h(t) = \frac{1}{L}\left[\mathcal{C}^{-1} * d_{err}(t) + \mathcal{A} * d_{ctrl}(t)\right]$$

$$h(t) = \frac{\Delta L_{free}}{L}$$

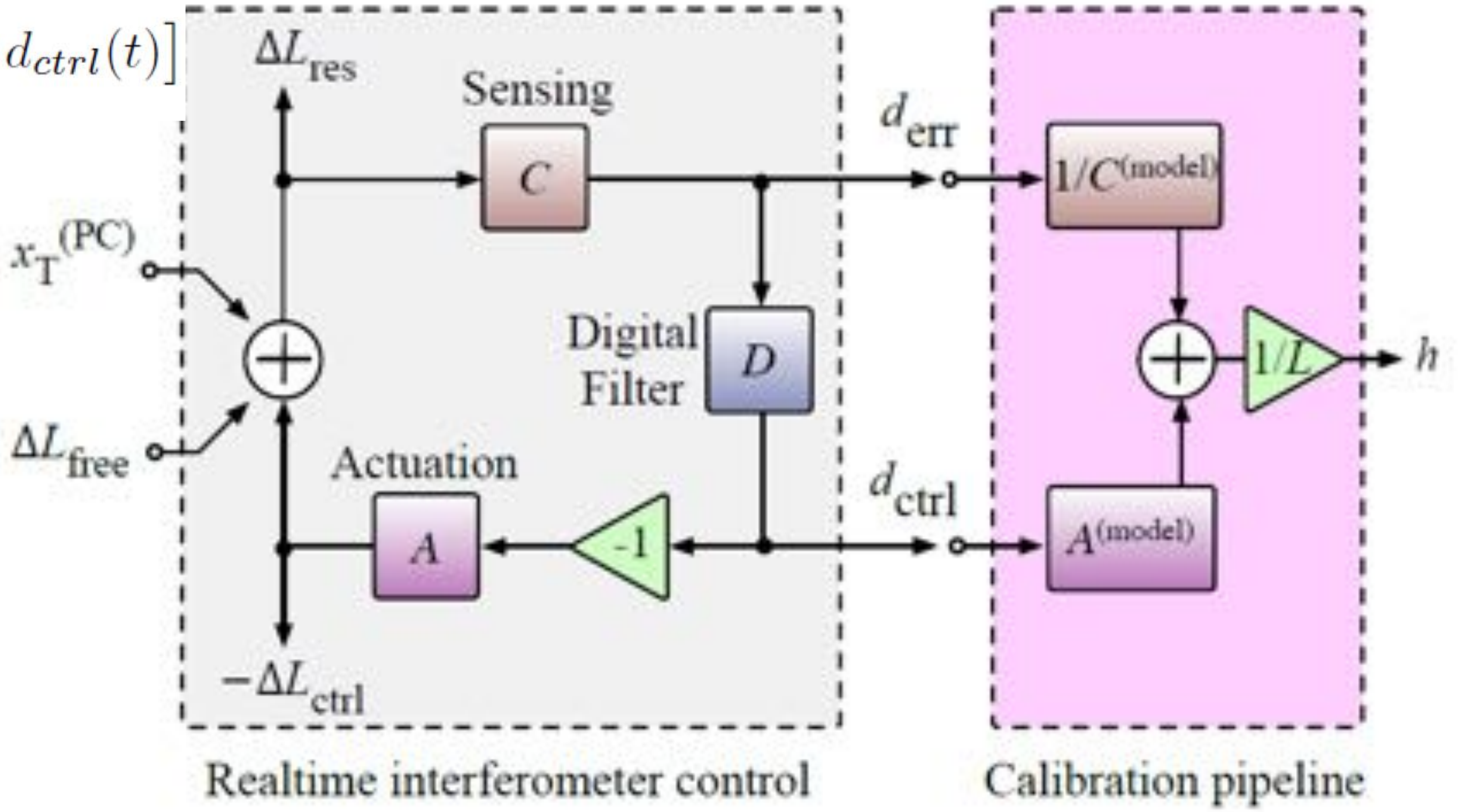

Noise model and likeihood

$$p(\mathbf{d}|\mathbf{h}) = \frac{1}{\det(2\pi\mathbf{C})^{1/2}} e^{-\frac{1}{2}\chi^2(\mathbf{d},\mathbf{h})}$$

$$\chi^2(\mathbf{d},\mathbf{h}) = \mathbf{r}\cdot\mathbf{C}^{-1}\cdot\mathbf{r} = (d_{Ik} - h_{Ik})C^{-1}_{(Ik)(Jm)}(d_{Jm} - h_{Jm})$$

$$(\mathbf{a}|\mathbf{b}) = 2\int_0^\infty \frac{\tilde{a}(f)\tilde{b}^*(f) + \tilde{a}^*(f)\tilde{b}(f)}{S_n(f)}\, df$$

$$p(\mathbf{d}|\boldsymbol{\theta}) = \exp\left(-\frac{1}{2}\sum_I \left[(\mathbf{d}_I - \mathbf{h}_I(\boldsymbol{\theta})|\mathbf{d}_I - \mathbf{h}_I(\boldsymbol{\theta})) + \int \ln(S_n^I(f))\, df\right]\right)$$

Signal detection

$$p(\mathbf{d} \mid \mathcal{H}_0) = p_0(\mathbf{d}) \quad \text{and} \quad p(\mathbf{d} \mid \mathcal{H}_1) = p_1(\mathbf{d})$$

$$p(\mathcal{H}_1 \mid \mathbf{d}) = \frac{p(\mathcal{H}_1)p_1(\mathbf{d})}{p(\mathcal{H}_0)p_0(\mathbf{d}) + p(\mathcal{H}_1)p_1(\mathbf{d})} = \frac{p_1(\mathbf{d})}{p_0(\mathbf{d})}\left[\frac{p_1(\mathbf{d})}{p_0(\mathbf{d})} + \frac{p(\mathcal{H}_0)}{p(\mathcal{H}_1)}\right]^{-1}$$

$$\Lambda(\mathbf{d}|\boldsymbol{\theta}) = \frac{p(\mathbf{d} \mid \mathcal{H}_1)}{p(\mathbf{d} \mid \mathcal{H}_0)} = \frac{p_1(\mathbf{d})}{p_0(\mathbf{d})}$$

Matched filter

$$\log \Lambda(\mathbf{d}|\boldsymbol{\theta}) = (\mathbf{d} \mid \mathbf{h}(\boldsymbol{\theta})) - \frac{1}{2}(\mathbf{h}(\boldsymbol{\theta}) \mid \mathbf{h}(\boldsymbol{\theta}))$$

Bayesian Method

- What we are doing?
  - Observe Gravitational Wave
  - Obtain series of electronic signal
  - Extract some numbers
- What we want?
  - What is the model parameter for the given data?
  - How probable those parameters?
  - How much believe those values?

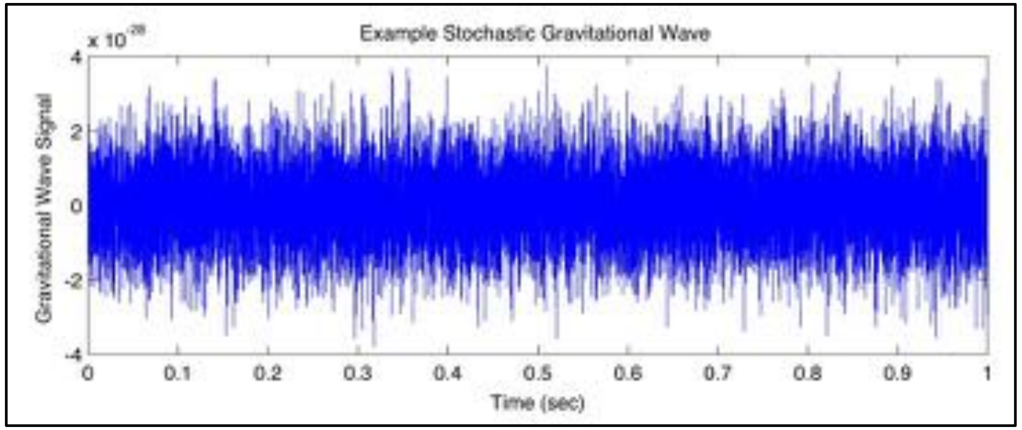

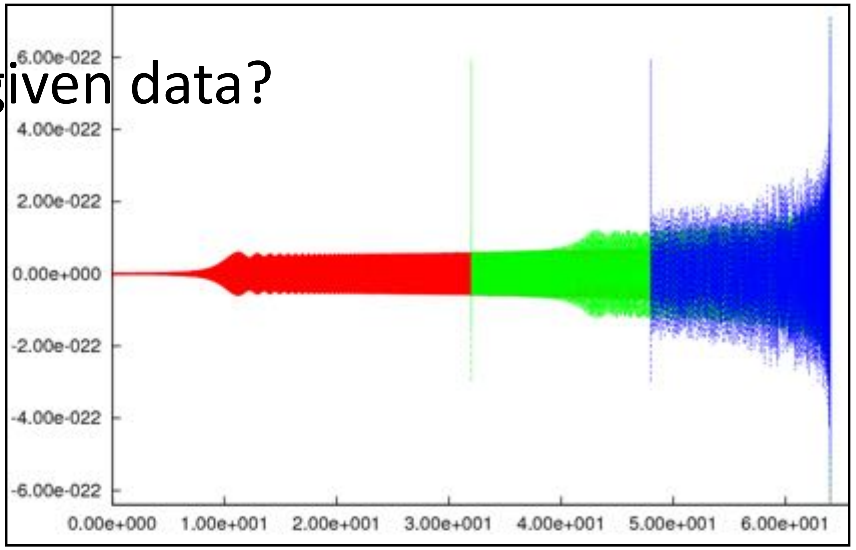

Bayesian Method

- Question: “What is the distribution of parameters for the given observed data?”

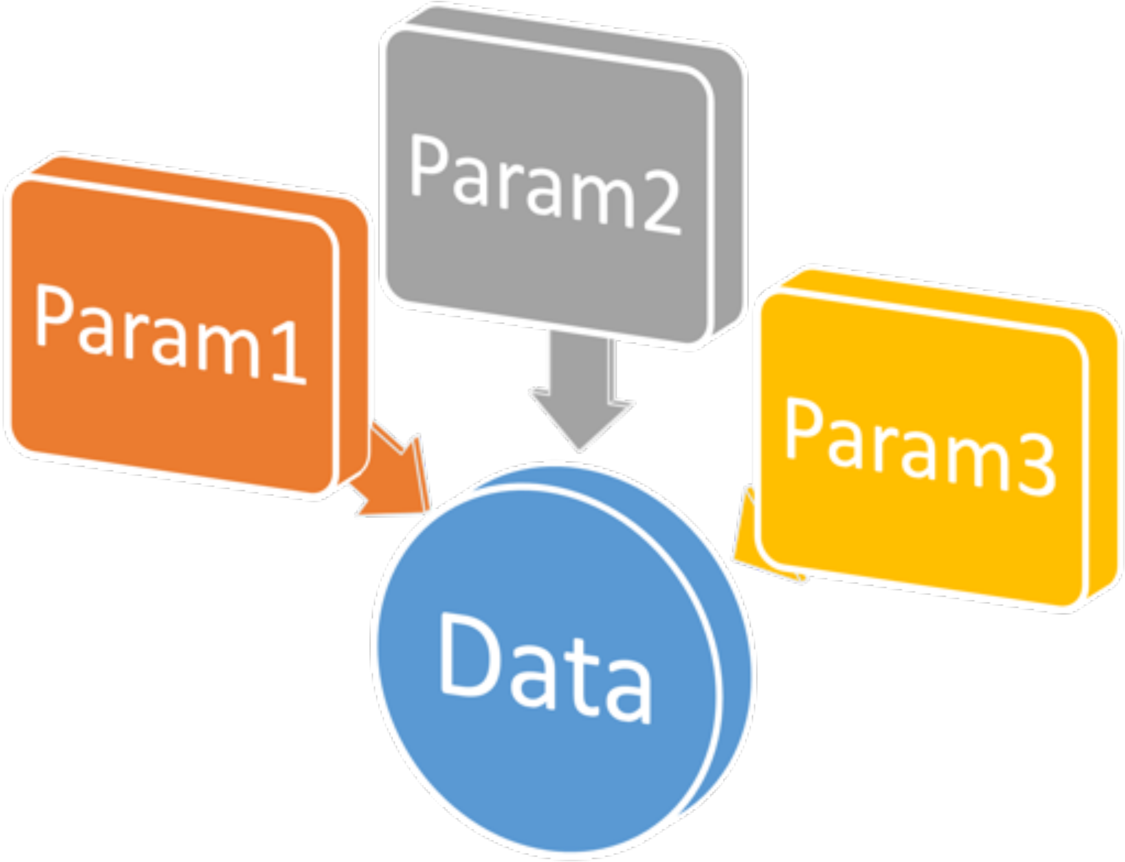

Parameter estimation

- Subtract signal model from data: $d - h(\vec{\lambda})$ where $d = h_{true} + n$
- Likelihood function for stationary Gaussian noise

$$\mathcal{L}(d|\vec{\lambda}) \propto e^{-\frac{1}{2}\left\langle d-h\left(\vec{\lambda}\right), d-h(\vec{\lambda})\right\rangle}$$

- Posterior probability of model parameters $\vec{\lambda}$ for given data d(Bayes' theorem):

$$p\left(\vec{\lambda}\middle|d, M\right) = \frac{p\left(\vec{\lambda}\middle|M\right)p(d|\vec{\lambda}, M)}{p(d|M)}$$

- Need models for signal/noise and specify prior knowledge

Priors

- the component masses m_1 and m_2;
- the spin vectors $\vec{S}_1$ and $\vec{S}_2$;
- the polarisation angle ψ and the angle θ_{jn} between the total angular momentum $\vec{J}$ and the propagation direction of the gravitational wave $\hat{n}$;
- the source luminosity distance D_L;
- the source right ascension α and declination δ;
- a reference phase φ_0 and a reference time, typically the gravitational-wave strain peak time, t_0.

Prior

- All physical priors are assumed to be 1 (a priori we do not know)
- Distance prior comes from volume integration factor $\int d^3\vec{r} = \int r^2 dr \sin\theta d\theta d\phi = \int r^2\, dr d\mu d\phi, \mu = \cos\theta$
- Mass prior comes from parameter space change $\int dm_1\, dm_2 = \int \frac{m_1 m_1}{m_c} dm_c\, dq = \int \frac{(m_1+m_2)^2}{(m_1-m_2)\eta^{-3/5}} dm_c d\eta$
- $\int r^2 dr d\mu d\phi = \int r^3 d\ln r\, d\mu d\phi$

$$\int \frac{m_1 m_1}{m_c} dm_c\, dq = \int \frac{(m_1+m_2)^2}{(m_1-m_2)\eta^{-3/5}} dm_c d\eta$$

distance prior

mass prior for mc and q

mass prior for mc and eta

PARAMETER ESTIMATION

Coherent Bayesian inference: $p(\vec{\theta}|\vec{d}) \propto p(\vec{d}|\vec{\theta}) \cdot p(\vec{\theta})$

The likelihood $p(\vec{d}|\vec{\theta})$ depends on

$$\langle s|h\rangle = 4\,\mathrm{Re}\int_0^\infty \frac{\tilde{s}(f)\,\tilde{h}^*(f)}{S_n(f)}\,df$$

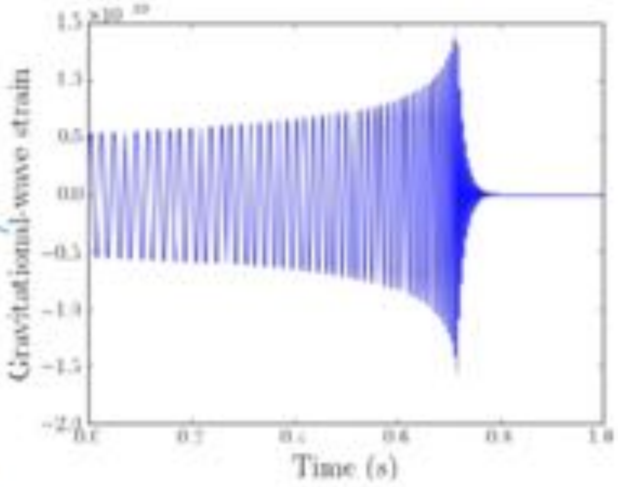

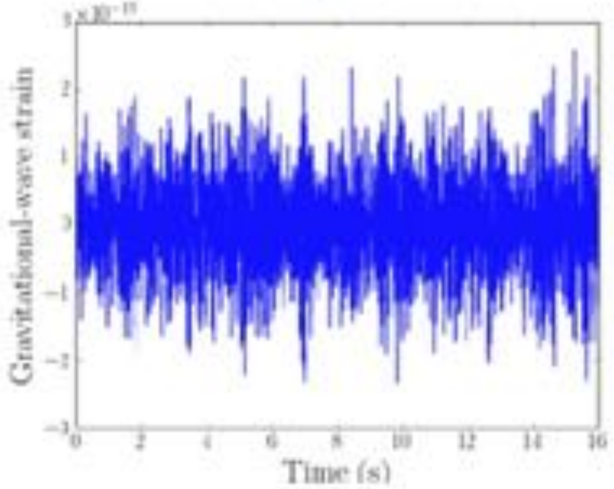

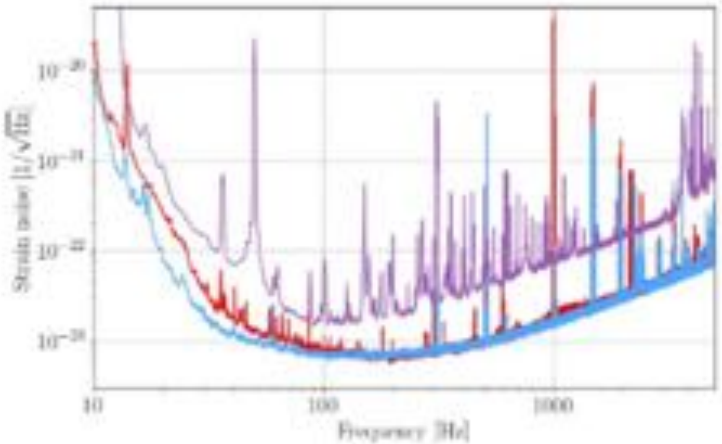

Metropolis-Hasting algorithm

- Generate proposed parameter : $\vec{\theta}_* \sim q(\vec{\theta}_i \to \vec{\theta}_*)$
- Sample from uniform distribution : $u \sim U(0,1)$
- Calculate Hasting ratio : $H = \frac{\pi(\vec{\theta}_*) q(\vec{\theta}_i \to \vec{\theta}_*)}{\pi(\vec{\theta}_i) q(\vec{\theta}_* \to \vec{\theta}_i)}$
- if $u < \min(1, H)$, then $\vec{\theta}_{i+1} = \vec{\theta}_*$
- else $\vec{\theta}_{i+1} = \vec{\theta}_i$
- For Gaussian proposal : $H = \frac{\pi(\vec{\theta}_*)}{\pi(\vec{\theta}_i)}$

Parallel Tempering

- Posterior at Temperature T
- $\pi(\vec{\theta}) = \mathcal{L}(\vec{\theta})^{1/T} P(\vec{\theta})$

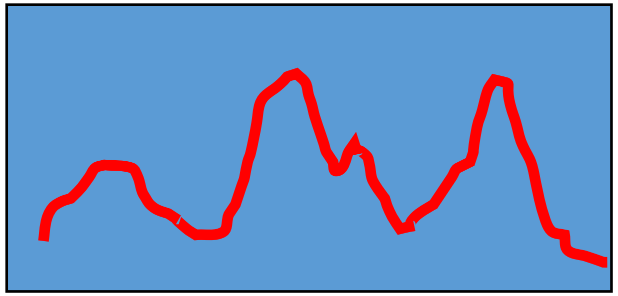

- Swapping ratio
- $SwapR = \left(\frac{\mathcal{L}(\vec{\theta}_2)_{T_2}}{\mathcal{L}(\vec{\theta}_1)_{T_1}}\right)^{\left(\frac{1}{T_1} - \frac{1}{T_2}\right)}$, $T_1 < T_2$
- Swap when $u < \min(1, SwapR)$

$T > 1$

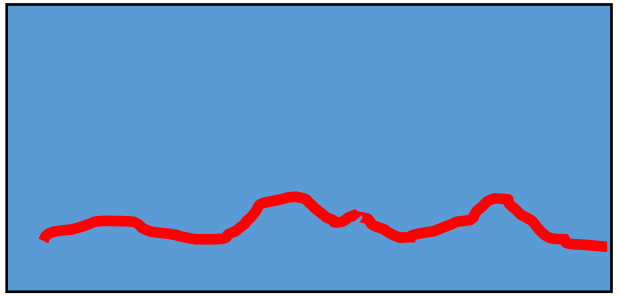

CBC waveform models

- BBH waveform models:
  - Effective one-body models(SEOBNRv4_ROM, SEOBNRv3)
  - Phenomenological models(IMRPhenomPv2)
  - Tuned to NR waveform in aligned spin sector
- BNS waveform models:
  - BBH models with phase correction from fit to NR(IMRPhenomPv2NRT, SEOBNRv4NRT)
  - Effective one-body models including tidal effects(SEOBNRv4T, TEOBResumS)
  - Post-Newtonian SPA waveform model (TaylorF2)

Inspiral waveform

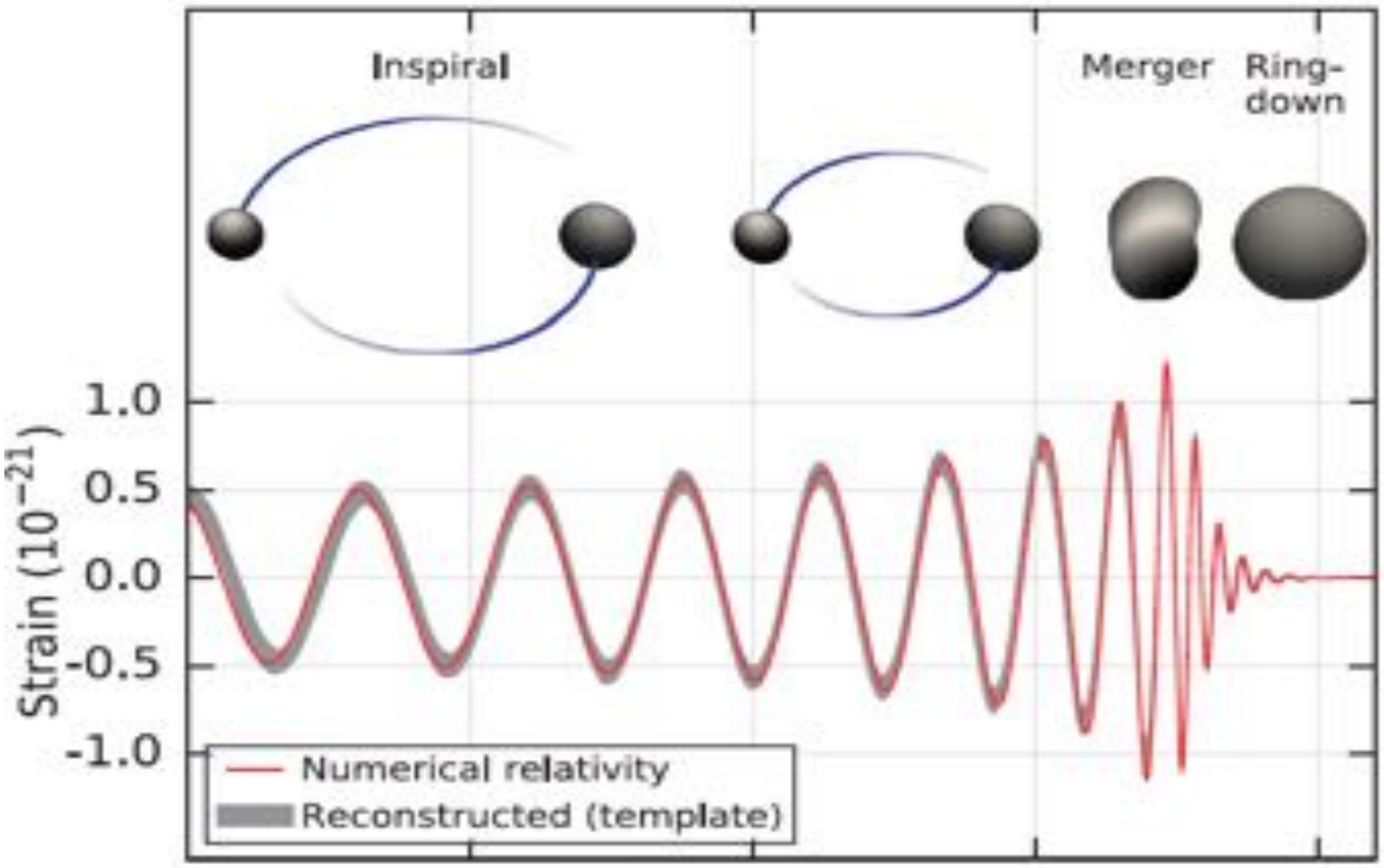

Model parameters

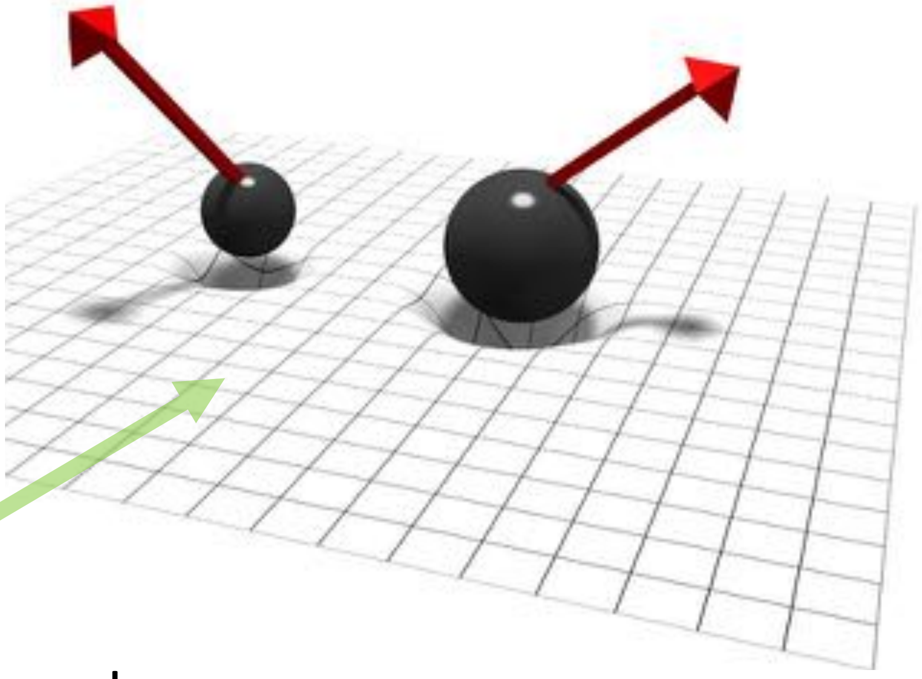

- Intrinsic parameters
  - masses, spins, tidal deformability, eccentricity
- Extrinsic parameters
  - time, sky position, distance, orientation, reference phase

$\hat{N}$

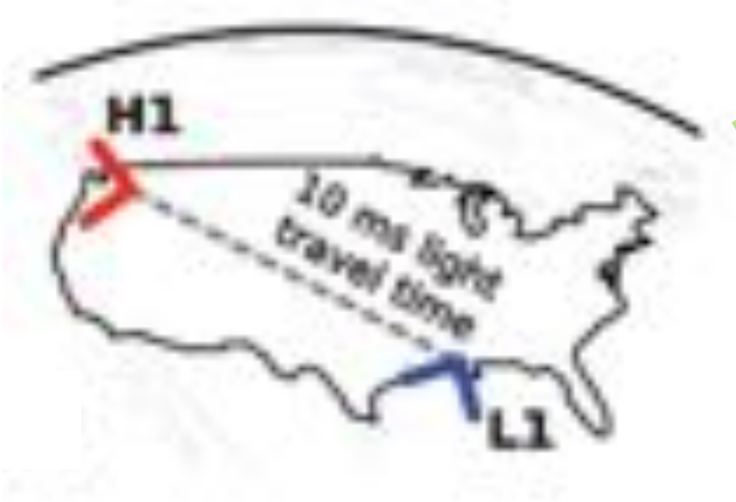

INTRINSIC PARAMETERS

$$\mathcal{M} = \frac{(m_1 m_2)^{3/5}}{(m_1+m_2)^{1/5}} = \left[\frac{q}{(1+q)^2}\right]^{3/5}(m_1+m_2)$$

Chirp mass – leading order PN expansion

$$q = \frac{m_2}{m_1} \le 1$$

Total mass 1PN but accessible through

$$f_{GW,max} = \frac{1}{6\sqrt{6}\,(2\pi)}\frac{c^3}{GM} \simeq 2.2\,\mathrm{kHz}\left(\frac{M_\odot}{M}\right)$$

$$\vec{\chi}_i = \frac{c\,\vec{S}_i}{G\,m_i^2} \qquad a_i = |\vec{\chi}_i| = \frac{c\,|\vec{S}_i|}{G\,m_i^2}$$

Dimensionless spin (spin-spin coupling 2PN)

$$\chi_{eff} = \frac{(m_1\vec{\chi}_1 + m_2\vec{\chi}_2)\cdot\vec{L}_N}{m_1+m_2}$$

Effective aligned spin (spin-orbit coupling 1.5PN)

$$\chi_p = \frac{1}{B_1 m_1^2}\max(B_1 S_{1\perp}, B_2 S_{2\perp})$$

Effective precession spin parameter (2PN)
arXiv:1308.3271

$$B_1 = 2 + \frac{3q}{2} \qquad B_2 = 2 + \frac{3}{2q}$$

BNS only

$$\Lambda = \frac{2}{3}k_2\left(\frac{c^2}{G}\frac{R}{m}\right)$$

Dimensionless tidal deformability

$$\tilde{\Lambda} = \frac{16}{13}\frac{(m_1+12m_2)m_1^4\Lambda_1 + (m_2+12m_1)m_2^4\Lambda_2}{M^5}$$

Effective tidal deformability parameter (5PN)

Parameter estimation results

Event	$m_1/M_\odot$	$m_2/M_\odot$	$\mathcal{M}/M_\odot$	χ_{eff}	$M_f/M_\odot$	a_f	$E_{rad}/(M_\odot c^2)$	$\ell_{peak}/(\mathrm{erg\,s^{-1}})$	d_L/Mpc	z	$\Delta\Omega/\mathrm{deg}^2$
GW150914	$35.6^{+4.8}_{-3.0}$	$30.6^{+3.0}_{-4.4}$	$28.6^{+1.6}_{-1.5}$	$-0.01^{+0.12}_{-0.13}$	$63.1^{+3.3}_{-3.0}$	$0.69^{+0.05}_{-0.04}$	$3.1^{+0.4}_{-0.4}$	$3.6^{+0.4}_{-0.4}\times10^{56}$	430^{+150}_{-170}	$0.09^{+0.03}_{-0.03}$	180
GW151012	$23.3^{+14.0}_{-5.5}$	$13.6^{+4.1}_{-4.8}$	$15.2^{+2.0}_{-1.1}$	$0.04^{+0.28}_{-0.19}$	$35.7^{+9.9}_{-3.8}$	$0.67^{+0.13}_{-0.11}$	$1.5^{+0.5}_{-0.5}$	$3.2^{+0.8}_{-1.7}\times10^{56}$	1060^{+540}_{-480}	$0.21^{+0.09}_{-0.09}$	1555
GW151226	$13.7^{+8.8}_{-3.2}$	$7.7^{+2.2}_{-2.6}$	$8.9^{+0.3}_{-0.3}$	$0.18^{+0.20}_{-0.12}$	$20.5^{+6.4}_{-1.5}$	$0.74^{+0.07}_{-0.05}$	$1.0^{+0.1}_{-0.2}$	$3.4^{+0.7}_{-1.7}\times10^{56}$	440^{+180}_{-190}	$0.09^{+0.04}_{-0.04}$	1033
GW170104	$31.0^{+7.2}_{-5.6}$	$20.1^{+4.9}_{-4.5}$	$21.5^{+2.1}_{-1.7}$	$-0.04^{+0.17}_{-0.20}$	$49.1^{+5.2}_{-3.9}$	$0.66^{+0.08}_{-0.10}$	$2.2^{+0.5}_{-0.5}$	$3.3^{+0.6}_{-0.9}\times10^{56}$	960^{+430}_{-410}	$0.19^{+0.07}_{-0.08}$	924
GW170608	$10.9^{+5.3}_{-1.7}$	$7.6^{+1.3}_{-2.1}$	$7.9^{+0.2}_{-0.2}$	$0.03^{+0.19}_{-0.07}$	$17.8^{+3.2}_{-0.7}$	$0.69^{+0.04}_{-0.04}$	$0.9^{+0.05}_{-0.1}$	$3.5^{+0.4}_{-1.3}\times10^{56}$	320^{+120}_{-110}	$0.07^{+0.02}_{-0.02}$	396
GW170729	$50.6^{+16.6}_{-10.2}$	$34.3^{+9.1}_{-10.1}$	$35.7^{+6.5}_{-4.7}$	$0.36^{+0.21}_{-0.25}$	$80.3^{+14.6}_{-10.2}$	$0.81^{+0.07}_{-0.13}$	$4.8^{+1.7}_{-1.7}$	$4.2^{+0.9}_{-1.5}\times10^{56}$	2750^{+1350}_{-1320}	$0.48^{+0.19}_{-0.20}$	1033
GW170809	$35.2^{+8.3}_{-6.0}$	$23.8^{+5.2}_{-5.1}$	$25.0^{+2.1}_{-1.6}$	$0.07^{+0.16}_{-0.16}$	$56.4^{+5.2}_{-3.7}$	$0.70^{+0.08}_{-0.09}$	$2.7^{+0.6}_{-0.6}$	$3.5^{+0.6}_{-0.9}\times10^{56}$	990^{+320}_{-380}	$0.20^{+0.05}_{-0.07}$	340
GW170814	$30.7^{+5.7}_{-3.0}$	$25.3^{+2.9}_{-4.1}$	$24.2^{+1.4}_{-1.1}$	$0.07^{+0.12}_{-0.11}$	$53.4^{+3.2}_{-2.4}$	$0.72^{+0.07}_{-0.05}$	$2.7^{+0.4}_{-0.3}$	$3.7^{+0.4}_{-0.5}\times10^{56}$	580^{+160}_{-210}	$0.12^{+0.03}_{-0.04}$	87
GW170817	$1.46^{+0.12}_{-0.10}$	$1.27^{+0.09}_{-0.09}$	$1.186^{+0.001}_{-0.001}$	$0.00^{+0.02}_{-0.01}$	≤ 2.8	≤ 0.89	≥ 0.04	$\geq 0.1\times10^{56}$	40^{+10}_{-10}	$0.01^{+0.00}_{-0.00}$	16
GW170818	$35.5^{+7.5}_{-4.7}$	$26.8^{+4.3}_{-5.2}$	$26.7^{+2.1}_{-1.7}$	$-0.09^{+0.18}_{-0.21}$	$59.8^{+4.8}_{-3.8}$	$0.67^{+0.07}_{-0.08}$	$2.7^{+0.5}_{-0.5}$	$3.4^{+0.5}_{-0.7}\times10^{56}$	1020^{+430}_{-360}	$0.20^{+0.07}_{-0.07}$	39
GW170823	$39.6^{+10.0}_{-6.6}$	$29.4^{+6.3}_{-7.1}$	$29.3^{+4.2}_{-3.2}$	$0.08^{+0.20}_{-0.22}$	$65.6^{+9.4}_{-6.6}$	$0.71^{+0.08}_{-0.10}$	$3.3^{+0.9}_{-0.8}$	$3.6^{+0.6}_{-0.9}\times10^{56}$	1850^{+840}_{-840}	$0.34^{+0.13}_{-0.14}$	1651

KAGRA may join to the end of O3

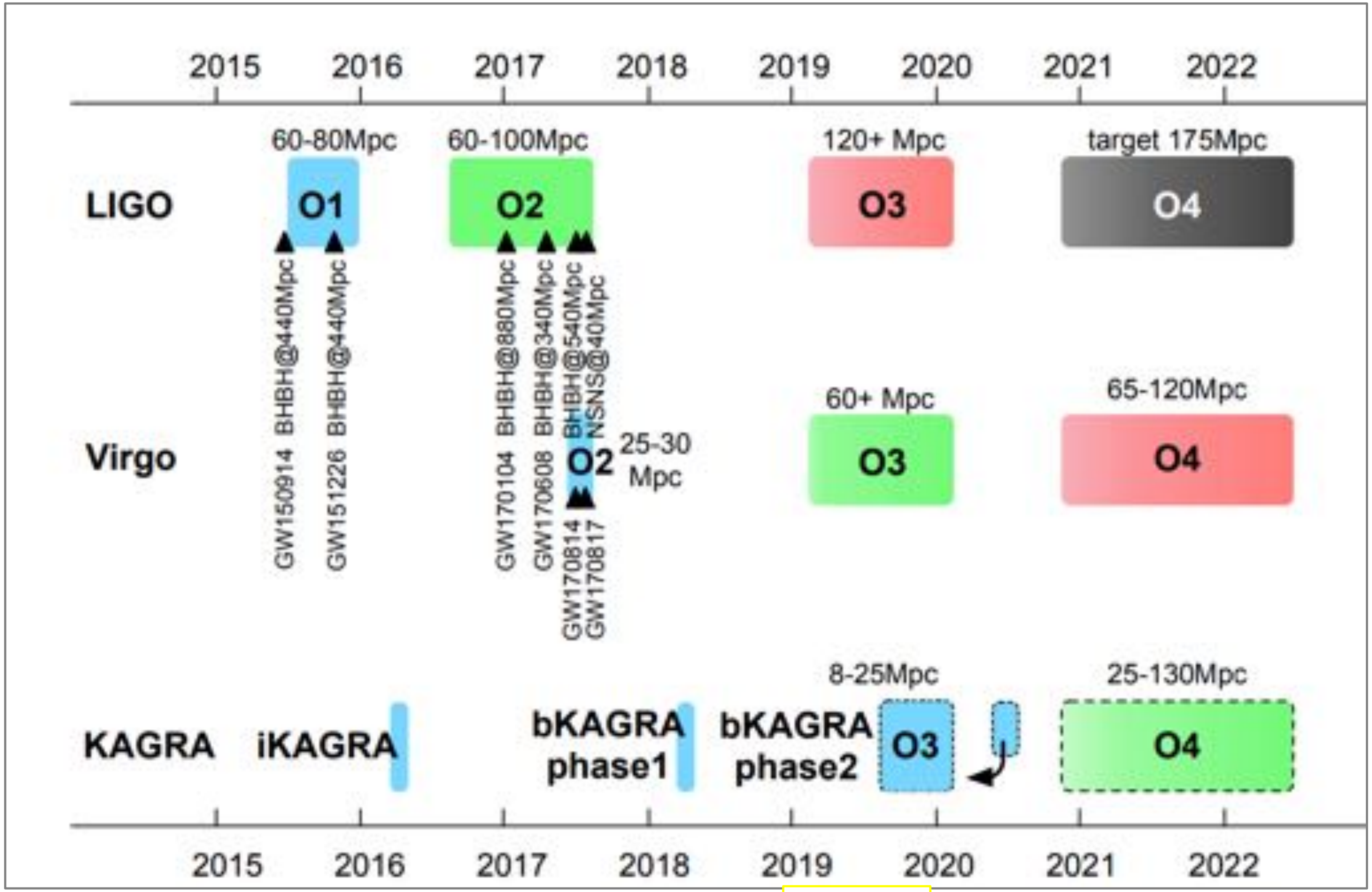

today

nature astronomy

Perspective | Published: 08 January 2019

KAGRA: 2.5 generation interferometric gravitational wave detector

https://arxiv.org/pdf/1811.08079.pdf

International Detector Network

Remarks

- Open gravitational wave observation era
- O1, O2 LIGO/Virgo have made 10 BBH and 1 BNS GW detections
- Approximately one GW detection per 15 days of data searched
- Merge rates determined
  - BNS: [110, 3840] $\mathrm{Gpc}^{-3}\mathrm{y}^{-1}$
  - BBH: [9.7, 101] $\mathrm{Gpc}^{-3}\mathrm{y}^{-1}$
  - NSBH merge rate 90% upper limit of 610(580) $\mathrm{Gpc}^{-3}\mathrm{y}^{-1}$
- O3 is started
- Four detectors: H1, L1, Virgo, KAGRA

Thank you